Environmental changes on North Iceland during the deglaciation and the Holocene: foraminifera, diatoms and stable isotopes

K. L. Knudsen [a], H. Jiang [a, b], E. Jansen [c], J. Eiríksson [d], J. Heinemeier [e] and M. -S. Seidenkrantz [a]

[a] Department of Earth Sciences, University of Aarhus, DK-8000, Aarhus C, Denmark
[b] Laboratory of Geographic Information Science, East China Normal University, Shanghai, 200062, PR China
[c] Bjerknes Centre for Climate Research and Department of Geology, Allégt. 55, N-5007, Bergen, Norway
[d] Science Institute, University of Iceland, IS-101, Reykjavik, Iceland
[e] The AMS [14]C Dating Laboratory, Institute of Physics and Astronomy, University of Aarhus, DK-8000, Aarhus C, Denmark

Abstract

A combined study of foraminifera, diatoms and stable isotopes in marine sediments off North Iceland records major changes in sea surface conditions since about 15800 cal years (yr) BP. Results are presented from two gravity cores obtained at about 400 m water depth from two separate sedimentary basins on each side of the submarine Kolbeinsey Ridge. The chronology of the sedimentary record is based partly on AMS ^{14}C dates, partly on the Vedde and the Saksunarvatn tephra markers, as well as the historical Hekla AD 1104 tephra. During the regional deglaciation, the planktonic foraminiferal assemblages are characterised by consistently high percentages of sinistrally coiled *Neogloboquadrina pachyderma*. However, major environmental variability is reflected by changes in stable isotope values and diatom assemblages. Low $\delta^{18}O$ values indicate a strong freshwater peak as well as possible brine formation by sea-ice freezing during a pre-Bølling interval (Greenland Stadial 2), corresponding to the Heinrich 1 event. The foraminifera suggest a strong concurrent influence of relatively warm and saline Atlantic water, and both the foraminifera and the diatoms suggest mixing of cold and warm water masses. Similar but weaker environmental signals are observed during the Younger Dryas (Greenland Stadial 1) around the level of the Vedde Ash. Each freshwater peak is succeeded by an interval of severe cooling both at the beginning of the Bølling–Allerød Interstadial Complex (Greenland Interstadial 1) and during the Preboreal, presumably associated with the onset of intense deep water formatiom in the Nordic Seas. The Holocene thermal optimum, between 10200 and about 7000 cal years (yr) BP, is interrupted by a marked cooling of the surface waters around 8200 cal yr BP. This cold event is clearly expressed by a pronounced increase in the percentages of sinistrally coiled *N. pachyderma*, corresponding to a temperature decrease of about 3°C. A general cooling in the area is indicated after 7000–6000 cal yr BP, both by the diatom data and by the planktonic foraminiferal data. After a severe cooling around 6000 cal yr BP, the planktonic foraminiferal assemblages suggest a warmer interval between 5500 and 4500 cal yr BP. Minor temperature fluctuations are reflected both in the foraminiferal and in the diatom data in the upper part of the record, but the time resolution of the present data is not high enough to pick up details in environmental changes through the late Holocene.

Author Keywords: Author Keywords: palaeoceanography; diatoms; foraminifera; stable isotopes; sediments; last 16000 years; North Atlantic

1. Introduction

Strong climatic gradients between the Arctic and the North Atlantic realms traverse the North Icelandic shelf, enhancing the significance of this key area for the study of oceanographic variability through the deglaciation and the Holocene. The shelf is located in a sensitive boundary region between Atlantic water, which is brought to the area by the relatively warm, high-salinity Irminger Current, and cold, low-salinity surface water of the East Icelandic Current (Fig. 1). The Arctic surface water of the East Icelandic Current is partly derived from the East Greenland Current (Polar water) and partly from westerly eddies of the Norwegian Atlantic Current (Atlantic water) (e.g. Stefansson, 1962; Johannesen, 1986; Swift, 1986; Malmberg and Jonsson, 1997 and Hansen and Østerhus, 2000).
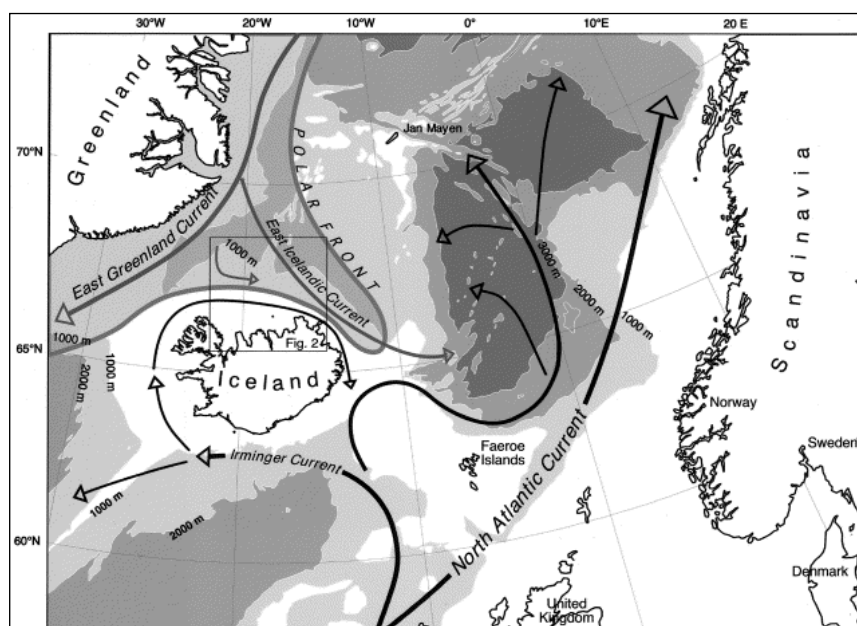

Fig. 1. The regional modern surface circulation around Iceland and the position of the marine Polar Front. Depth contour intervals 1000 m (modified after Knudsen and Eiríksson, 2002 and Hurdle, 1986, Map A8). The extent of Fig. 2 is indicated by a box.

The strength of the North Atlantic Current is generally related to deep water formation in the Nordic Seas, which is again associated with southward overflow across the Greenland–Iceland–Faeroe–Scotland Ridge. The North Atlantic Current is expected to be strong during active deep water formation, and weak during periods of freshening of the surface waters north of Iceland, i.e. during periods with strong input of Polar water from the East Greenland Current and the East Icelandic Current. At present the Norwegian Sea Deep Water (NSDW) replaces the mixed surface water masses at about 3–400 m depth off North Iceland (Fig. 2 and Fig. 3). During periods of strong overflow in the Denmark Strait and across the Iceland–Faeroe Ridge, the cold deep water masses (NSDW) may be expected to influence the topographic basins north of Iceland (Eiríksson et al., 2000a).
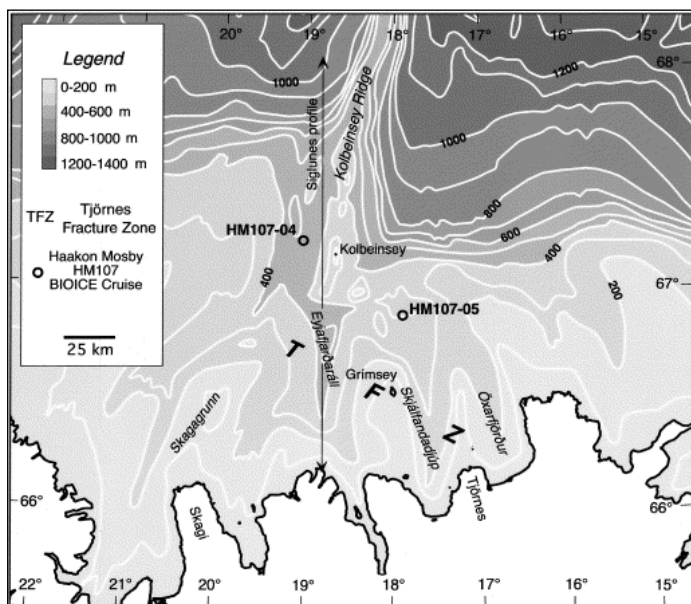
Fig. 2. Location of the core sites north of Iceland (contour intervals 100 m). The arrow indicates the location of the oceanographic section on Fig. 3. Abbreviation: TFZ, Tjörnes Fracture Zone.
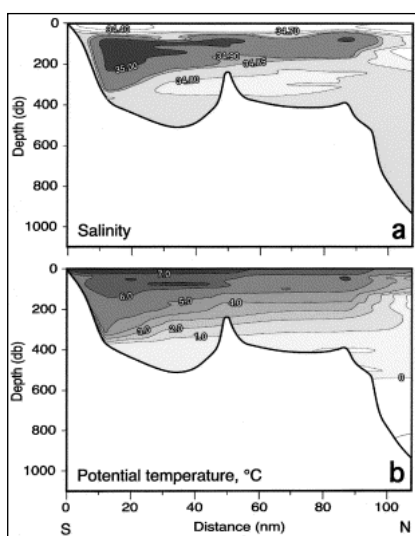

Fig. 3. Oceanographic section from the north coast of Iceland towards north across the shelf to the slope (the Siglunes profile). Summer salinity (a) and temperature (b) data (August 1998) are presented as an example of the distribution of water masses. The oceanography is based on data from the Iceland Marine Institute (Hedinn Valdimarsson, pers. commun.; see Oceanographic Group Homepage, http://www.hafro.is/hafro/Sjora/index.htm). Abbreviations: db, decibar≈1 m; nm, nautical mile. (After Knudsen and Eiríksson, 2002.)

The modern summer sea surface temperature in the study area is relatively constant, generally around 6–7°C, while the winter sea surface temperature is around 1–3°C (Jiang et al., 2002). These temperatures were lower during past cold periods when the East Icelandic Current had an increased East Greenland Current component, while warmer and more saline waters were brought into the area during periods of relatively stronger influence of the Irminger Current (e.g. Eiríksson et al., 2000a; Andrews et al., 2001a and Andrews and Giraudeau, 2002). Consequently, past changes in the position of the oceanic Polar Front across the North Icelandic shelf can be registered in the sedimentary record of the region. This has previously been demonstrated both for the areas around Iceland (e.g. Koç et al., 1993; Sarnthein et al., 1995 and Voelker et al., 1998) and from the shelf west of Iceland (Jennings et al., 2000) as well as north of Iceland (Andrews et al., 2000; Eiríksson et al., 2000a; Eiríksson et al., 2000b and Andrews et al., 2001a). Consistency between marine late Holocene proxies from the North Icelandic shelf and atmospheric and terrestrial data from the Greenland ice sheet and from Iceland glacier advances shows that there is a close relationship between the oceanic system and the atmospheric circulation in the region (Eiríksson et al., 2000b; Andrews et al., 2001b; Andrews et al., 2001c; Andrews and Giraudeau, 2002 and Jiang et al., 2002).

The seafloor of the North Icelandic shelf is characterised by the Tjörnes Fracture Zone featuring numerous active basins in a mud dominated environment (Fig. 2). The sedimentary record of the two gravity cores HM107-05 and HM107-04 (Fig. 2), extending back to almost 15800 cal yr BP, represents part of the deglaciation as well as the entire Holocene. Local and temporal variability in sedimentation rates are observed on each side of the ridge. A high sedimentation rate is recorded during the Lateglacial and the Preboreal in core HM107-05 east of the ridge (mean=48 cm/1000 yr), probably reflecting proximity of glacial and glaciomarine processes. This was followed by reduced Holocene rates (mean=12.5 cm/1000 yr) east of the ridge, while the sedimentation rate was higher in core HM107-04 west of the ridge (mean=33 cm/1000 yr). As the eastward flow of the Irminger Current along the outer shelf is parallel to the depth contours, the Kolbeinsey Ridge forms a barrier favouring deposition of bed load silts on its westward side where the currents are slowed down and deflected across the ridge.

The purpose of this paper is to present high resolution planktonic foraminifera, stable isotope and diatom evidence of variable sea surface conditions off North Iceland through the Lateg1acial and across the Pleistocene–Holocene transition, and a lower resolution record for the Holocene. Benthic foraminiferal species and sedimentary data are included when important for the environmental interpretation. An overview of benthic foraminiferal distribution and sedimentological data in a lower time resolution study of the same two cores was previously published by Eiríksson et al. (2000a).

The chronostratigraphy in this study is based on a combination of well-known tephra markers and a series of AMS ^{14}C dates. The record is discussed in terms of the Greenland ice-core events (Björck et al., 1998; Walker et al., 1999 and Lowe et al., 2001), but for reason of clarity, the classic chronostratigraphical terminology of Mangerud et al. (1974) is indicated as well.

2. Materials and methods

Two gravity cores, HM107-05 (66°54′08″N, 17°54′19″W; water depth 396 m, core length 394.3 cm) and HM107-04 (67°13′38″N, 19°03′00″W; water depth 458 m, core length 392.7 cm) from the North Icelandic shelf (Fig. 2), were obtained in 1995 on the HM107 BIOICE cruise with RV *Haakon Mosby*, 90 and 120 km offshore (see also Eiríksson et al., 2000a). The cores are located on each side of the Kolbeinsey Ridge.

2.1. Foraminifera

The foraminiferal samples generally represent 1-cm sediment slices, and analyses are carried out at intervals varying between 1 and 10 cm (the time resolution varies between 15 and a maximum of 1200

years). The samples were washed through 1000-, 125- and 63-μm sieves, according to the methods described by Feyling-Hanssen et al. (1971) and Knudsen (1998). The foraminifera were concentrated from the 125–1000-μm dry fraction of sediment by means of the heavy liquid C_2Cl_4 (specific gravity 1.6 g cm^{-3}). At least 300 specimens of planktonic as well as benthic specimens were analysed in the 125-μm fraction, when possible. In some intervals the number of planktonic specimens was relatively low, and samples containing less than 30 specimens were excluded from the statistics. The Preboreal sediments were generally very poor in foraminifera, especially from the planktonic group. Some of the samples from this interval were, therefore, supplemented with neighbouring 1-cm sediment slices up to an aggregate thickness of 3 cm. For taxonomic notes, see Appendix A.

2.2. Diatoms

Each diatom sample represents a 1-cm sediment slice, and analyses were carried out at intervals of 5 or 10 cm. All the samples were treated with 10% HCl to remove the calcareous matter, washed with distilled water, and treated with 30% H_2O_2 (1–2 h in a water bath at 60°C) in order to destroy the organic material. Diatom slides were made by using Naphrax (dn=1.73). In all 102 samples were analysed (51 samples for each core). More than 300 diatoms valves were counted in each sample (excluding *Chaetoceros* resting spores), although at some levels the limited amount of diatoms in the sediments prevented reaching this figure. In general, the diatoms were well preserved. Diatom assemblage zones were identified using the cluster analysis technique of Grimm (1987). For taxonomic notes, see Appendix B.

2.3. Stable isotopes

Stable isotopes were measured on the planktonic sinistrally coiled *Neogloboquadrina pachyderma* as well as on the benthic species *Islandiella norcrossi* from the 125–1000-μm fraction of each foraminiferal sample, when possible. For intervals with sparse contents of *I. norcrossi* the benthic species *Cassidulina neoteretis* was measured instead. The data set was supplemented by a series of overlapping samples with measurements of both benthic species. This made it possible to normalise the $\delta^{18}O$ values of *C. neoteretis* to *I. norcrossi* (correction factor +0.69±0.29). All the $\delta^{18}O$ values presented in the diagrams are corrected for the ice volume effect, using the Fairbanks (1989) sea-level curve as dated by Bard (1990) with a correction of 0.11‰ $\delta^{18}O$ per 10 m sea-level change (subtracted from the measured $\delta^{18}O$ values). The stable isotopes were measured on a Finnigan MAT 251 mass spectrometer at the Stable Isotope Laboratory, University of Bergen. Results are given with respect to PeeDee Belemnite, after calibration to the National Institute of Standard and Technology NBS 19 standard.

2.4. Sediments

The basic sedimentological properties of cores HM107-05 and HM107-04 were published by Eiríksson et al. (2000a), including grain size, carbonate content, water content, shear strength, mineralogical composition and tephra geochemistry. The present paper, therefore, only presents an overview of the lithology, shown on a depth scale in Fig. 4 and Fig. 5 together with important tephra markers as well as ice rafted debris (IRD) contents. We also include some additional grain size parameters, pebble content and higher resolution mineralogical data.
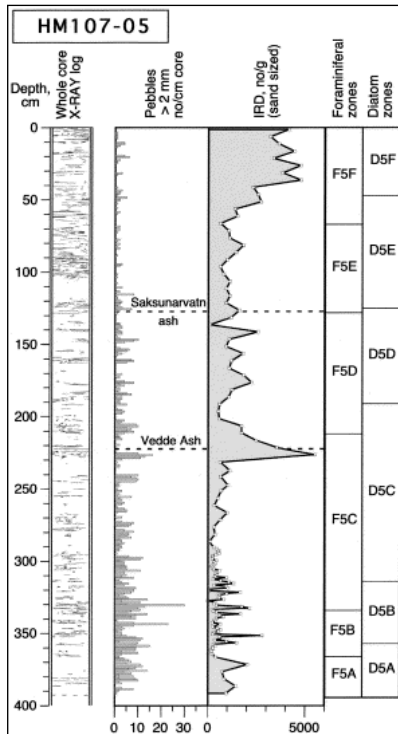

Fig. 4. Lithology of core HM107-05 based on X-ray photographs, and mineralogical analyses. The whole-core X-ray logs show laminations and structures drawn after the X-ray negatives. Pebbles >2 mm in diameter are shown as frequency per cm core length. For definition and discussion of IRD, see text. Benthic foraminiferal biozones (from Eiríksson et al., 2000a) and diatom biozones (this paper) are indicated, as well as the level of the Vedde and Saksunarvatn tephras (stippled lines).
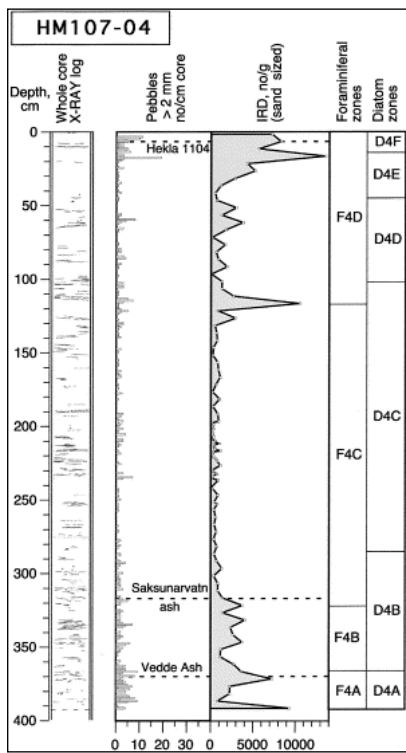
Fig. 5. Lithology of core HM107-04 based on X-ray photographs, and mineralogical analyses. The level of the Vedde and Saksunarvatn tephras and the historical Hekla AD 1104 tephra marker are indicated (stippled lines). See also caption of Fig. 4.

Sorting (standard deviation) was calculated using moment statistics (McBride, 1971), and the sortable silt percentage and mean were calculated as the percentage of the 10–63-μm fraction out of the total fines and the mean grain size of that fraction (McCave et al., 1995).

The pebble content and specific mineralogical components are used as proxies for sedimentation from melting ice in the waters north of Iceland. The number of clasts over 2 mm in diameter was counted on whole-core X-ray negatives, and the number of pebbles per 1-cm-sediment thickness in the core was calculated. This method may underestimate the pebble frequency when two or more pebbles coincide in core depth and exposure direction, but the generally very low concentration of pebbles in both cores is considered to reduce this potential error.

For the study of mineralogical provenance, at least 300 grains were identified and counted in the >125-μm sand fraction of the sieved sample. This grain size interval has been used in previous studies of IRD content in the Nordic Seas (e.g. Henrich et al., 1995). Most of the allochtonous, non-volcanic sand grains fall into three groups: crystals (mainly quartz and feldspar), rock fragments (plutonic and sedimentary), and altered or abraded volcanic fragments. A substantial portion of the first two groups must originate outside Iceland, the reworked volcanics may have Icelandic or Greenlandic provenance. It is considered most likely that the sand grains with provenance outside Iceland were transported and released to the North Icelandic shelf by sea-ice and icebergs from Greenland and the Arctic Ocean. Some of the potentially local sand grains may have become incorporated in sea-ice through eolian, coastal or shelf processes. Statistically, however, the flux of the three mineralogical groups is positively (r ranging from 0.35 to 0.75) and significantly ($P<0.0005$ in all cases) correlated in both cores, and each group can be used to predict the other two. This supports the interpretation that all three groups share a common origin, and can be considered to represent IRD. Substantial coastal sea-ice cover may enhance eolian transport of sand to the middle and outer shelf. The IRD flux was calculated as the product of the mass accumulation rate (as defined by van Andel et al., 1975) and the number of IRD grains per gram sediment.

3. Chronology

The chronology for this work is based on combined tephrochonology and AMS ^{14}C datings of either molluscs or benthic or planktonic foraminifera. Most of the AMS ^{14}C dates have previously been published by Eiríksson et al. (2000a), who also presented an age–depth model based on ^{14}C ages (uncalibrated) for each of the two cores. A standard marine reservoir correction of 400 years was used throughout the entire record by Eiríksson et al. (2000a). For the age model of this paper, all the ^{14}C dates have been calibrated with CALIB4 (Stuiver et al., 1998a). The marine model calibration curve with $\Delta R=0$, corresponding to a reservoir correction of approximately 400 years (Stuiver et al., 1998b; see also Andersen et al., 1989), has been used for the Holocene record, while a reservoir correction of 800 years ($\Delta R=400$) has been applied for older samples (Table 1, Table 2, Table 3 and Table 4). The present-day reservoir age of the coastal waters of Iceland is consistent with the $\Delta R=0$ value, and Eiríksson et al. (2000a) did show that a $\Delta R=0$ value is also applicable at the level of the Saksunarvatn ash (9000 ^{14}C yr BP), whereas a reservoir correction of 750–800 years was necessary at the Vedde Ash level (10300 ^{14}C yr BP). Clearly, a change of reservoir age took place in the waters north of Iceland between the deposition of the Vedde and the Saksunarvatn tephras, close to the Pleistocene–Holocene boundary.

Table 1. Radiocarbon datings and tephra markers in core HMI07-05, calibrated with CALIB4 (Stuiver et al., 1998a) using the marine model calibration curves (Stuiver et al., 1998b)

HM107-05, depth (cm)	Laboratory No.	Material/dated tephra layer	^{14}C age (BP) ±1 s	Cal age(s) BP (R=400)	Cal ±1 s (BP)	Cal age(s) BP (R=800)	Cal ±1s (BP)	δ^{13}C
18–19	AAR-3381	Foraminifera, total benthic fauna	2 015 ±45	1 560	1 620–1 520			−1,1
49–51	AAR-4117	Foraminifera, total benthic fauna	5 050 ±45	5 430	5 460–5 320			−0,9
122–125	AAR-4419	Foraminifera, total benthic fauna	9 190 ±80	9 820	9 930–9 620			−1,7
125–128	AAR-4420	Foraminifera, total benthic fauna	9 250 ±70	9 840	10 260–9 730			−1,4
127		**Saksunarvatn ash**		**10 200**				
137–141	AAR-3380	Foraminifera, total benthic fauna	9 730 ±60	10 330	10 600–10 300			−1,1
212–213	AAR-3382	Foraminifera, total benthic fauna	10 900±100	12 570–12 340	12 800–11 770	11 620–11 400	11 910–11 160	−1,1
222		**Vedde Ash**		**12 000**				
224–227	AAR-4118	Foraminifera, *Neoglob. pach.* sin.	10 970±60	12 610–12 370	12 810–12 150	11 660	11 910–11 370	+0,3
224–228	AAR-4119	Foraminifera, total benthic fauna	11 090±80	12 800–12 650	12 880–12 370	11 920–11 750	12 280–11 590	−0,5
228–231	AAR-3379	Foraminifera, total benthic fauna	11 440±90	12 980	13 130–12 870	12 780–12 630	12 870–12 340	−0,8
331–334	AAR-4116	Foraminifera, total benthic fauna	12 920±80	14 350	15 290–14 180	14 070	14 270–13 710	−1,3
364–366	AAR-4115	Foraminifera, total benthic fauna	13 560±90	15 700	15 950–15 480	15 300	15 510–14 380	−1,2
379.5–381	AAR-3377	Foraminifera, *Neoglob. pach.* sin.	13 790±120	15 970	16 240–15 710	15 520	15 760–15 280	−1,1
380–381	AAR-3378	Foraminifera, total benthic fauna	14 010±120	16 230	16 490–15 970	15 760	16 020–15 520	−0,9

379.5–381	AAR-5377	Foraminifera, Neoglob. pach. sin.	13790±120	15970	16240–15710	15520	15780–15280	−1.1
380–381	AAR-3378	Foraminifera, total benthic fauna	14010±120	16230	16490–15970	15760	16020–15520	−0.9
393–394.3	AAR-3375	Foraminifera, Neoglob. pach. sin.	14100±140	16330	16610–16060	15870	16140–15600	−1.3
393–394.3	AAR-3376	Foraminifera, total benthic fauna	13690±100	15860	16110–15610	15430	15630–14480	−1.2
393–394.3	AAR-3383	Molluscs, Yoldiella lenticula, Thyasira gouldi	13980±90	16190	16440–15950	15730	15970–15500	−1.3

A standard reservoir correction of ca. 400 years (ΔR=0) is built into this model for samples younger than 10000 ^{14}C yr, while ca. 800 years (ΔR=400) has been used for older samples. The datings were carried out at the AMS ^{14}C Dating Laboratory, University of Aarhus, Denmark.

Table 2. Age–depth model boundaries for core HM107-05 and sedimentation rates for each linear segment of the model

Top (cm)	Base (cm)	Base (cal BP)	Sedimentation rate (cm/kyr)	Base, boundary type
0	18.5	1560	12	Age zone boundary (AMS date)
18.5	50	5430	8	Age zone boundary (AMS date)
50	67	6430	16	Zone F5F/F5E boundary
67	127	10200	16	Age zone boundary, Saksunarvatn ash
127	128	10220	50	Age zone boundary, Zone F5D/F5E boundary
128	212	11470	336	Age zone boundary, Zone F5C/F5D boundary
212	222	12000	19	Age zone boundary, Vedde Ash
222	229.5	12400	19	Age zone boundary
229.5	334	14130	60	Age zone boundary, Zone F5B/F5C boundary
334	366	15320	27	Age zone boundary, Zone F5A/F5B boundary
366	394.3	15740	64	Core base

The ages of the benthic foraminiferal biozone boundaries (major faunal changes) are indicated. Ages of diatom zone boundaries are entered in the text (see also Fig. 6).

Table 3. Radiocarbon datings and tephra markers in core HMI07-04

HMI07-04, depth (cm)	Laboratory No.	Material/dated tephra layer	^{14}C age (BP) ±1 s	Cal age(s) BP (R=400)	Cal ±1 s (BP)	Cal age(s) BP (R=800)	Cal ±1 s (BP)	δ^{13}C
7		**Hekla 1104**		**850**				
87–88	AAR-4202	Mollusc, Siphonodentalium lobatum	5345±55	5700	5750–5630			+1.7
142–143	AAR-5040	Mollusc, Thyasira equalis	6340±70	6780	6880–6720			0°
165–166	AAR-2932	Molluscs, Thyasira equalis, Yoldiella sp.	6830±60	7360	7410–7280			−2.0
207–208	AAR-4203-2	Mollusc, Siphonodentalium sp.	7700±100	8160	8280–8020			+1.3
211–212	AAR-5743	Molluscs, Thyasira gouldi, Yoldiella lenticula	7350±90	7790	7910–7700			0°
269–270	AAR-5745	Mollusc, Siphonodentalium lobatum	8790±45	9400–9110	9600–9070			+1.2
292–293	AAR-3384	Mollusc, cf. Siphonodentalium lobatum	9075±60	9790	9840–9550			+1.0
308–313	AAR-5103	Foraminifera, total benthic fauna	9415±65	10290–10140	10250–9860			−1.7
317		**Saksunarvatn ash**		**10200**				
362–366	AAR-5194	Foraminifera, total benthic fauna	10540±45	11650	11910–11360	11110–10850	11290–10840	−1.1
369–371	AAR-4421	Foraminifera, total benthic fauna	11100±80	12800–12650	12890–12370	11930–11750	12280–11670	−0.3
369–371	AAR-4422	Foraminifera, Neoglob. pach. sin.	10980±90	12620–12380	12810–12150	11670	11930–11360	+0.1
370		**Vedde Ash**		**12000**				
371–373	AAR-4424	Foraminifera, Neoglob. pach. sin.	11160±90	12820–12670	12900–12630	12080–11960	12340–11700	+0.1
371–373	AAR-4423	Foraminifera, total benthic fauna	11290±110	12890	12980–12660	12330	12800–11760	−0.7
391–392.7	AAR-4418	Foraminifera, total benthic fauna	12040±80	13470	13800–13400	13140	13730–13010	−0.6

0°= not measured (standard value assumed). See also caption of Table 1.

Table 4. Age–depth model boundaries for core HMI07-04. See caption of Table 2

Top (cm)	Base (cm)	Base (cal BP)	Sedimentation rate (cm/kyr)	Base, boundary type
0	6.5	850	8	Age zone boundary, Hekla 1104 tephra
6.5	87.5	5700	17	Age zone boundary (AMS date)
87.5	117	6300	49	Zone F4C/F4D boundary
117	207.5	8160	49	Age zone boundary (AMS date)
207.5	317	10200	54	Age zone boundary, Saksunarvatn ash
317	322	10290	56	Zone F4B/F4C boundary
322	366	11110	54	Top of hiatus, base Zone F4B
366	366	11800		Base of hiatus, top Zone F4A
366	370	12000	20	Age zone boundary, Vedde Ash
370	392.7	13140	20	Core base

See also Fig. 7.

Several studies from the northern North Atlantic have previously shown higher reservoir age values for the Lateglacial than observed at present (e.g. Austin et al., 1994; Bard et al., 1994; Haflidason et al., 1995 and Bondevik et al., 2001). Waelbroeck et al. (2001) have presented data showing that the reservoir age was not constant during the Lateglacial, amounting to 930±250 yr during the Younger Dryas, but as much as 1880±750 yr at the end of the Heinrich 1 event (14500 cal yr BP). Both Bondevik et al. (2001) and Waelbroeck et al. (2001) found that the reservoir ages were comparable to the present-day values during the warm Bølling–Allerød period. Taking these variations into account is not straightforward, however, as additional complications may well have been introduced by anti-phase relationships between the water masses of the North Icelandic shelf region and those of the eastern North Atlantic during the Lateglacial. We have therefore chosen to adopt a ΔR=400 value for age calibration of all samples older than 10000 ^{14}C yr BP.

The age–depth models of HM107-05 and HMI07-04 are shown in Fig. 6 and Fig. 7 (Table 1 and Table 3). The age models were constructed by means of age zones that are delimited by tephra markers,

[14]C dates and biozone boundaries. Sedimentation rate for each age zone has been obtained with linear interpolation (Table 2 and Table 4). Ice-core ages are used for the Vedde (12000 cal yr BP) and the Saksunarvatn (10200 cal yr BP) tephras (Grönvold et al., 1994; Zielinski et al., 1997 and Gulliksen et al., 1998). The historical Hekla AD 1104 has simply been converted to cal yr BP. In the absence of constraining dates, we have chosen to let sedimentation rates change at benthic foraminiferal biozone boundaries. This is based on the assumption that major faunal changes are considered to coincide with changes in sedimentation rates because they reflect palaeoceanographic changes in the region (see also Eiríksson et al., 2000a). In the age models, zero age is assumed for the core tops, based on correlation with corresponding box cores with intact core tops. In core HMl07-04, AMS ^{14}C dates from the base of biozone F4B and the top of F4A indicate an hiatus of almost 700 years between those two biozones, coinciding with a level of major faunal changes (see Eiríksson et al., 2000a).
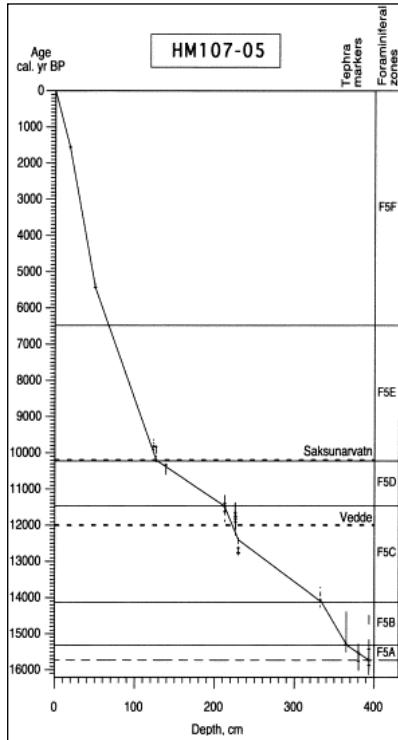

Fig. 6. Age–depth diagram for core HM107-05. Tephra markers and AMS ^{14}C datings, based on molluscs and foraminifera (Table 1), are used as a basis for the reconstruction of linear segments in the age–depth model (see also text and Table 2). The age calibration is based on Stuiver et al., 1998a and Stuiver et al., 1998b. A standard reservoir correction of about 400 years (ΔR=0) is built into this model for the marine samples younger than 10000 ^{14}C years, while a reservoir correction of about 800 years (ΔR=400) has been used for older samples (± one standard deviation is indicated by error bars). An age of 12000 cal yr BP is applied for the Vedde Ash and 10200 cal yr BP for the Saksunarvatn ash. The ages of benthic foraminiferal zone boundaries are given in Table 2.
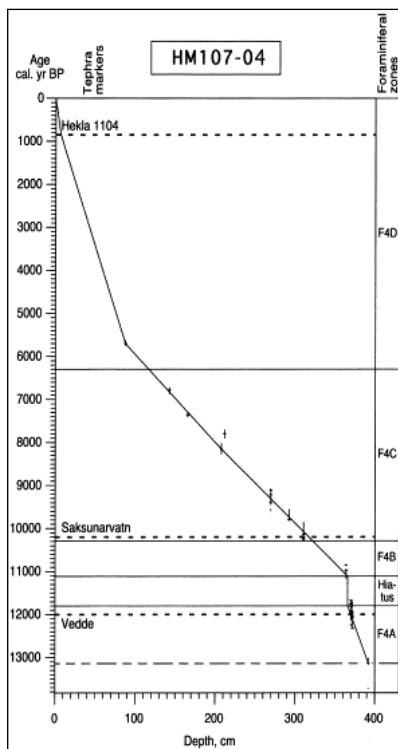

Fig. 7. Age–depth diagram for core HM107-04. Tephra markers, including the historical Hekla AD 1104, and AMS ^{14}C datings, based on molluscs and foraminifera (Table 3), are used as a basis for the reconstruction of linear segments in the age–depth model (see also text and Table 4). An hiatus between 11800 and 11110 cal yr BP is shaded (see also text). The ages of benthic foraminiferal zone boundaries are given in Table 4. See also caption of Fig. 6.

4. Lithology

The origin of sand-sized tephra particles in cores HMl07-05 and HMl07-04 is primarily attributed to volcanic events in Iceland (Eiríksson et al., 2000a). The sand fraction constitutes up to 40%, but is generally less than 20% of the sediment. The dispersal of volcanic material from Iceland is considered to be largely wind-driven with sand-sized and finer grained air-fall tephras settling conformably on the shelf seafloor. Local eruptions may have formed submarine or subaerial eruption plumes and caused tephra deposition from suspension or submarine turbidity currents across local basins (Lackschewitz et al., 1994). Mineralogical analyses have revealed a relatively high background of sand-sized reworked tephra. This was attributed to occasional storm reworking of local shallow water deposits on the Kolbeinsey Ridge by Eiríksson et al. (2000a). Rock fragments and minerals of 'crustal' origin, as well as rounded and altered volcanic fragments were interpreted as IRD. The provenance of the mud fraction has not been examined. Both ice rafting and volcanic processes have undoubtedly contributed to the fines, in addition to benthic organic activity, redeposition by bottom currents and

suspension deposition of material carried to the shelf environment by eolian and fluvial processes, as well as organic processes in the water column.

There is a distinct relationship between mean grain size (Eiríksson et al., 2000a) and sortable silt content, indicating that the bulk of the sediment volume has been deposited by decelerating bottom currents. During periods of weak bottom currents, the sedimentation was dominated by deposition of fine silt and clay from suspension, but during periods of stronger currents carrying sortable silt, the mean grain size was pushed up. On the freshly split core surfaces and X-ray images of both cores, the predominantly silty sediments appear faintly streaky due to grain size variations within the silt range. This is consistent with deposition from suspension and concomitant weak bottom currents. Distinct bedding is confined to tephra layers and rare coarse sandy or pebbly units. Bioturbation was only observed sporadically as isolated burrow marks.

The pebble content (Fig. 4 and Fig. 5) at both sites displays roughly three intensity levels. Below the Vedde Ash, the average pebble content amounts to 5 pebbles/cm core, fluctuating between 0–30. The average value decreases to 2, fluctuating between 0–10, in the interval between the Vedde and the Saksunarvatn tephras, and the average post-Saksunarvatn value is 1 pebble/cm core. However, a marked increase is observed in the uppermost 20 cm of core HM107-04, indicating increased ice rafting north of Iceland in the last 2000 years of the Holocene.

5. Planktonic foraminifera and stable isotopes

The percentage distributions of selected taxa of planktonic foraminifera in cores HM107-05 and HM107-04 are shown on Fig. 8 and Fig. 9 together with the stable isotopic records for the planktonic and the benthic foraminifera, as well as the IRD fluxes.
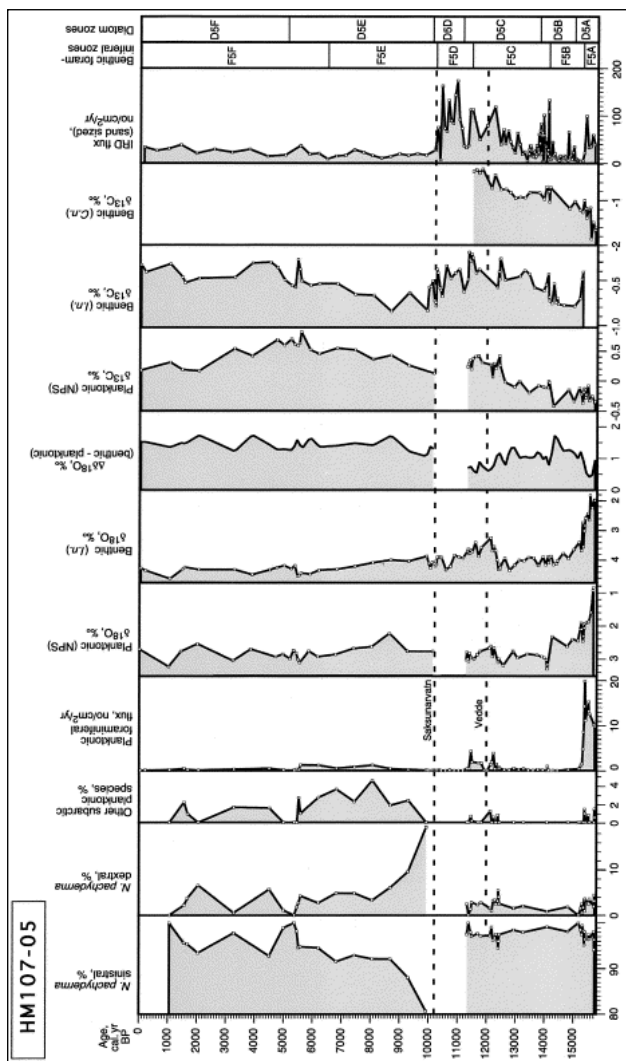

Fig. 8. Percentage distribution (calculated from total planktonic contents) of selected species and species groups of planktonic foraminifera, as well as the planktonic foraminiferal flux (number/cm^2/yr) in core HM107-05, shown on a calibrated age scale. Other subarctic planktonic species include the following species: *Turborotalita quinqueloba*, *Globigerina bulloides* and *Globigerinita glutinata*. The δ^{18}O (corrected for ice volume effect) and δ^{13}C curves are shown for the planktonic *Neogloboquadrina pachyderma* sinistral (NPS) and for the benthic *Islandiella norcrossi* (*I.n.*) and *Cassidulina neoteretis* (*C.n.*). *C. neoteretis* has been normalised to *I. norcrossi* values for the benthic δ^{18}O curve. The difference between benthic and planktonic δ^{18}O values is calculated by interpolation of fixed 100 years distances between data points. The IRD flux (sand-sized) is shown as number/cm^2/yr. The ages of the tephra markers (Vedde and Saksunarvatn) are shown with stippled lines. For comparison, the benthic foraminiferal zonation and the diatom zonation are also shown. For stratigraphical correlation, see Fig. 15.
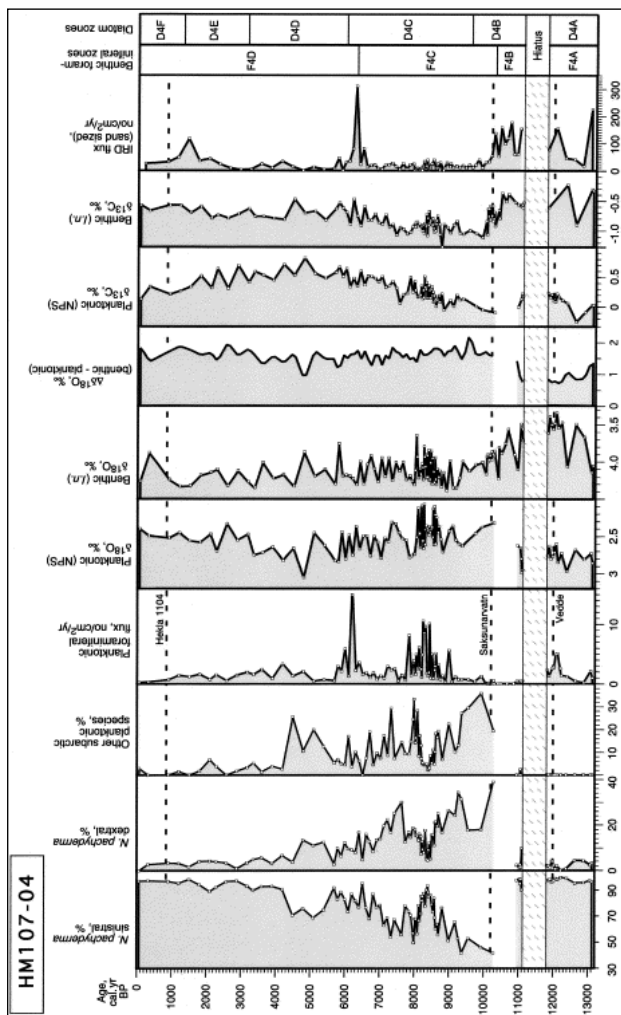
Fig. 9. Environmental data for core HM107-04. The ages of the tephra markers (Vedde, Saksunarvatn and Hekla 1104) are shown with stippled lines. The hiatus between 11800 and 11110 cal yr BP is shaded. For stratigraphical correlation, see Fig. 15. See also caption of Fig. 8.

5.1. Core HM107-05

5.1.1. The Lateglacial interval (15740–11500 cal yr BP)

There is a very high dominance of the arctic sinistrally coiled *Neogloboquadrina pachyderma* (mostly 95–100% of the total planktonic assemblage) throughout the Lateglacial part of core HM107-05 (Fig. 8). Other planktonic species are rare but include some specimens of dextrally coiled *N. pachyderma*, specifically in the lowermost part of the core (before about 15300 cal yr BP, i.e. in pre-Bølling time) and on both sides of the Vedde tephra horizon. This corresponds to intervals of increased planktonic foraminiferal fluxes, which would also indicate temporal changes in the water mass distribution in the area. An increased input of Atlantic water from the Irminger Current during these intervals has been assumed to be the explanation for these changes (see also Eiríksson et al., 2000a).

A very light planktonic oxygen isotope signal in the bottom part of the core presumably indicates a marked freshwater input to the surface waters in the area, which appears to continue into the Bølling–Allerød, almost until 14000 cal yr BP. Similar low isotopic values in the benthic curve suggest a mixing of surface and bottom waters. These coupled signals are most likely due to sea-ice freezing processes (Veum et al., 1992; Vidal et al., 1998 and Dokken and Jansen, 1999). Therefore, it is concluded on the basis of the oxygen isotope values that bottom water produced by brine formation probably influenced the core site, specifically before 15300 cal yr BP, but presumably also during the early part of the Bølling–Allerød complex and during the Younger Dryas. Similarities between the planktonic and benthic carbon isotope records also indicate active exchange between surface and bottom waters during most of the time span covered by the cores.

A strong influence of the benthic species *Cassidulina neoteretis*, combined with a high percentage of the high-salinity group Miliolida in pre-Bølling deposits on the North Icelandic shelf, has previously been related entirely to a temporary strong influence of Atlantic waters brought to the area by the Irminger Current (Eiríksson et al., 2000a). A similarly high influence of *C. neoteretis* has, however, also been registered during Heinrich events (and related to brine formation) in the North Atlantic by Lassen et al. (in press). The present isotopic data, combined with the faunal indication and a high biological production, reflected both in the planktonic and the benthic foraminiferal fluxes, suggest that the area was probably influenced both by freezing processes and a high input of Irminger Current water in the subsurface layers. The marked difference in faunal indication of the surface water masses compared to the bottom waters strongly suggests that the Irminger water influenced the subsurface and bottom waters much more than the surface waters.

It is interesting to notice that a similar, but less pronounced decrease in oxygen isotope values also occurs just before the Vedde tephra horizon and continues to the end of the Younger Dryas (11500 cal yr BP). This coincides with another marked maximum of *Cassidulina neoteretis*, lasting for a maximum of 800 years according to the present age model, a value which is presumably too high due to increased tephra input, influencing the age model during this time period (Fig. 12). This interval presumably represents another sea surface freshwater peak, combined with brine formation as well as increased Atlantic water inflow to the subsurface and bottom waters.

5.1.2. The Holocene interval (11500 cal yr BP to the present)

Only very few planktonic foraminifera were found in the Preboreal interval, but a low density fauna is present from about 10000 cal yr BP to the present time. Since rather few samples were analysed in this interval, the results only give an overview of the general trend in climate change. The percentage of sinistrally coiled *Neogloboquadrina pachyderma* is high, generally above 90% of the fauna, but there is a clear indication of warmer surface water conditions just after 10000 cal yr BP. After 7000–6000 cal yr BP, the percentages of sinistrally coiled *N. pachyderma* increase to more than 95%. This shows that Arctic or Polar water masses become predominant again (see Johannesen et al., 1994).

The planktonic $\delta^{18}O$ values fluctuate around 3‰ through the entire interval from 10000 cal yr BP to the present, while there is a clear increasing trend in the benthic values from 4 to about 4.4‰ between 10000 and around 5000 cal yr BP, and the benthic values fluctuate around that level throughout the late Holocene. The increasing difference between benthic and planktonic values in the late Holocene indicates an increasing stratification of the water column.

There is also a Holocene trend in the carbon isotope values of core HM107-05, with low values in the early Holocene and more positive values in the mid- to late Holocene intervals. This may be the general interglacial trend due to changes in the carbon cycle, which occurs in many cores in the Nordic Seas both in the Holocene and in Marine Isotope Substage 5e (e.g. Vogelsang, 1990 and Fronval and Jansen, 1997), but the resemblance with the trend towards more cold water dominance in the planktonic foraminiferal fauna (Fig. 8) would indicate that it may be due to a diminishing influence of Atlantic water and stronger dominance of the Arctic water domain with its higher $\delta^{13}C$ values (Johannesen et al., 1994). The somewhat reduced planktonic values towards the top of the cores may be due to a further influence of Polar waters, which have lower $\delta^{13}C$ values. This is corroborated by the concurrent highest values of the polar foraminiferal taxon *Neogloboquadrina pachyderma* sinistral and indication of increased IRD flux.

5.2. Core HM107-04

5.2.1. The Lateglacial interval (13140–11800 cal yr BP, i.e. base hiatus)

The Lateglacial interval in core HM107-04 is represented by relatively few samples, covering less than 1400 years. The percentage of *Neogloboquadrina pachyderma* sinistral is very high (95–100% of the total planktonic assemblage; Fig. 9). There is an increase both in planktonic and benthic foraminiferal fluxes just below the Vedde Ash (see also Eiríksson et al., 2000a), and the values continue at a relatively high level after that marker horizon. A decrease in both planktonic and benthic oxygen isotope values is also seen around the level of the Vedde Ash.

Even though the data from this interval are sparse, they strongly support the results from core HM107-05. The benthic faunal composition shows a pattern similar to the one described for core HM107-05, with an interval of high percentages of *Cassidulina neoteretis* on both sides of the Vedde Ash. In core HM107-04 this is associated with a maximum in the high-salinity group Miliolida. The isotope records and the faunal indications suggest that the surface waters at this site were probably also influenced by freezing processes during part of the Younger Dryas, and that there was an increased Atlantic water influx to the subsurface and bottom waters.

5.2.2. The Holocene interval (11110 cal yr BP, i.e. top hiatus to the present)

Only very few samples from the Preboreal (at around 11000 cal yr BP) contained enough planktonic foraminifera for interpretation. However, the high percentages of sinistrally coiled *Neogloboquadrina pachyderma* show that Arctic or Polar surface waters did predominate. The planktonic oxygen isotope values decrease from 3 to 2.6‰ within this short interval. The benthic oxygen isotope values fluctuate through the Preboreal, but with a general increase from ca. 3.5‰ at 11000 cal yr BP to ca. 4.0‰ around the level of the Saksunarvatn ash (10200 cal yr BP). The benthic foraminiferal assemblages, however, indicate increasing temperatures through the Preboreal interval (Eiríksson et al., 2000a).

The planktonic foraminiferal assemblages show that the highest surface water temperatures were reached between 10200 and 7000 cal yr BP at this core site, but with a generally decreasing trend. The percentages of sinistrally coiled *Neogloboquadrina pachyderma* increased from less than 50 at the beginning to 80–90% towards the end of the Holocene climatic optimum. The relatively warm period was, however, interrupted by a marked cooling between ca. 8600 and 8000 ca1 yr BP, when percentages of sinistrally coiled *N. pachyderma* increased to a maximum of 95%. This corresponds to a temperature decrease of about 3°C (see Johannesen et al., 1994). After a short period with relatively high influence of subpolar species between about 5500 and 4500 cal yr BP, the amount of sinistrally coiled *N. pachyderma* remains constantly high through the late Holocene, indicating the predominance of Arctic or Polar surface waters in the area.

The planktonic oxygen isotope values fluctuate, but display an increasing trend through the Holocene climatic optimum. Values as low as 2.1–2.2‰ are reached during the cooling event between 8600 and 8000 cal yr BP. These low values presumably indicate the influence of low-salinity surface waters in the area. There is a clear decrease in planktonic oxygen isotope values through the last 5000 cal years.

Benthic oxygen isotope values display a slight general increase through the Holocene, indicating a minor cooling trend of about 1°C. There is a clear increase from the Preboreal to the remaining Holocene, which would indicate that brine water influences the oxygen isotope signal until 10000 cal yr BP. The increase in the benthic to planktonic difference at the same time would tend to underscore this conclusion.

As observed for core HMl07-05, reduced planktonic δ^{13}C values towards the top of this core may be due to influence of Polar waters with its lower δ^{13}C values, an assumption which is supported by the high values of the polar sinistrally coiled form of *Neogloboquadrina pachyderma*.

6. Diatoms

A recent study of the modern distribution of diatoms in surface sediments around Iceland demonstrated a close relationship between diatom assemblages and the modern distribution of water masses (Jiang et al., 2001). These results, coupled with previous diatom research in the North Atlantic form the basis of the environmental interpretation of the diatom results presented in Fig. 10 and Fig. 11, which show the percentage distribution of the most common diatom taxa in cores HMl07-05 and HMl07-04. A brief summary of the most important environmental indicators is given below as it forms the background for the interpretation of the diatom results.
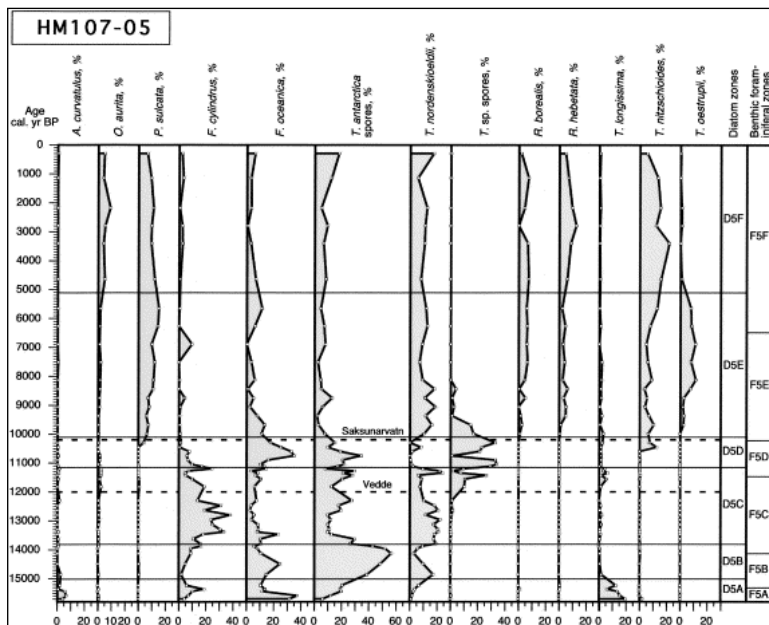

Fig. 10. Diatom distribution in core HM107-05 on a calibrated time scale. Frequencies are shown as percentages of the total assemblage (excluding *Chaetoceros* resting spores). Ages of zone boundaries are given in the text. For comparison, the benthic foraminiferal zonation is shown as well (ages of zone boundaries in Table 2). For stratigraphical correlation, see Fig. 15. The ages of the tephra markers (Vedde and Saksunarvatn) are shown with stippled lines.
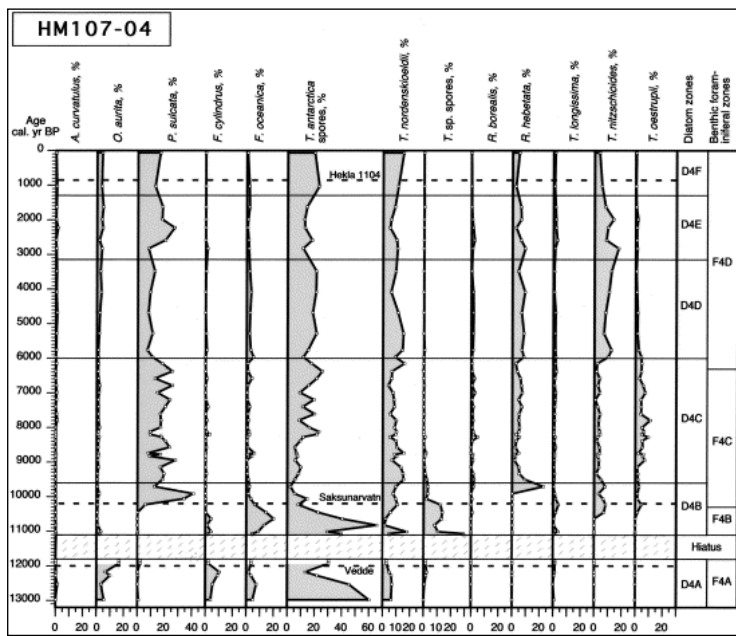
Fig. 11. Diatom distribution in core HM107-04. For ages of the benthic foraminiferal zone boundaries, see Table 4. The ages of the tephra markers (Vedde, Saksunarvatn and Hekla 1104) are shown with stippled lines. For stratigraphical correlation, see Fig. 15. See also caption of Fig. 10.

A strong influence of the Irminger Current on the North Icelandic shelf is indicated by *Thalassiosira oestrupii*, which is the main diatom species of the Atlantic assemblage in the modern warm North Atlantic water mass with salinities higher than 35.3 and sea surface temperatures above 3°C (Koç Karpuz and Schrader, 1990). In modern assemblages around Iceland, it is mainly found in the surface sediments south and west of Iceland, where the warm Irminger Current has a strong impact today (Jiang et al., 2001). The presence of the Irminger Current is also indicated by *Thalassionema nitzschioides* and *Paralia sulcata*, which constitute the main species of the Norwegian–Atlantic Current assemblage in the Greenland–Iceland–Norwegian seas (Koç Karpuz and Schrader, 1990). Both species are associated with the Atlantic waters flowing into the Skagerrak–Kattegat in the eastern North Atlantic (Jiang, 1996). They are mainly found in the modern surface sediments south and west of Iceland, where the Irminger Current has a strong impact (Jiang et al., 2001).

One of the most important taxa in the cold-water diatom assemblage associated with the cold, low-salinity East Icelandic Current is *Thalassiosira antarctica* resting spores (Jiang et al., 2001). It is one of the main taxa of the Arctic water assemblage, which at present coincides geographically with the seasonally sea-ice covered Iceland Plateau with salinity between 34.7 and 34.9 and temperatures ranging from freezing to 8°C (Koç Karpuz and Jansen, 1992).

Sea-ice conditions are indicated by *Fragilariopsis cylindrus*, which is bipolar in distribution, and *F. oceanica*, which is an arctic and/or sea-ice species (Hasle and Syvertsen, 1997). Both species are the main components of the sea-ice diatom assemblage in surface sediments from the seafloor around Iceland (Jiang et al., 2001). An assemblage containing *F. cylindrus*, *F. oceanica* and *Thalassiosira nordenskioeldii* was considered to be indicator of the spring bloom associated with melting ice in modern Bering Sea assemblages (Sancetta, 1981).

Mixed water masses are indicated by *Thalassiosira nordenskioeldii* and *Thalassiothrix longissima*. *Thalassiosira nordenskioeldii* is characteristic of modern diatom assemblages in areas influenced by a mixing of the warm Irminger Current and the cold waters of the East Icelandic Current north of Iceland. *Thalassiothrix longissima* is abundant (as the main species of the taxon *Thalassiothrix* spp.) in the modern surface sediments west of Iceland (Jiang et al., 2001). It is also associated with the West Greenland Current (De Séve, 1999), and it is very common in the North Atlantic, extending to the northern Arctic (Hustedt, 1930–1960 and Hendey, 1964). It is the main component of the Arctic–Norwegian waters mixing assemblage, which coincides with areas of mixture between the Arctic and the Atlantic waters (Koç Karpuz and Schrader, 1990).

Stratified water masses are inferred by abundant *Thalassiosira* sp. resting spores. The taxonomy of *Thalassiosira* sp. resting spores is unclear (Hasle, pers. commun.). It was only found in small amounts in a few modern surface samples north of Iceland (Jiang et al., 2001). Off North Iceland it only occurs in the interval from about 11500–9500 cal yr BP, where it is usually one of the dominant taxa. It was also recorded (as *Thalassiosira* cf. *scotia* resting spore, which is morphologically close to the present one) from Younger Dryas sediments in the Skagerrak–Kattegat in the eastern North Atlantic, where the water masses were highly stratified with high-salinity bottom waters and more brackish surface waters (Jiang et al., 1997). Therefore, we suggest that abundance of *Thalassiosira* sp. resting spores north of Iceland may reflect a local environment of highly stratified water masses rather than low sea surface temperature.

6.1. The Lateglacial and the Pleistocene–Holocene transition

6.1.1. Zone D5A, HM107-05 (15740–15000 cal yr BP)

This zone is dominated by *Fragilariopsis oceanica* and *Thalassiothrix longissima* together with *Fragilariopsis cylindrus*, *Thalassiosira antarctica* resting spores and *Actinocyclus curvatulus* (Fig. 10) indicating periodic seasonal ice cover in the oceanographic mixing zone between the cold East Greenland Current and the Irminger Current. A mixing of the two water masses in the area is shown by the co-occurrence of sea-ice species and the relatively warm species *T. longissima*.

6.1.2. Zone D5B, HM107-05 (15000–13800 cal yr BP)

There is a rapid decrease in *Fragilariopsis cylindrus* and *Thalassiothrix longissima* in this zone, and *Thalassiosira antarctica* resting spores become the most important component (Fig. 10). This change in assemblage suggests that a major change in the current pattern occurred at around 15000 cal yr BP. The East Icelandic Current had a major influence on the area during the time interval represented by zone D5B.

6.1.3. Zone D5C, HM107-05 (13800–11150 cal yr BP); Zone D4A, HM107-04 (13140–11800 cal yr BP, i.e. base hiatus)

These zones are characterised by abundant *Fragilariopsis cylindrus* and *Thalassiosira nordenskioeldii* with a rapid decline of *Thalassiosira antarctica* resting spores (Fig. 10 and Fig. 11), but they also contain a few relatively warm taxa such as *Thalassiothrix longissima*, *Odontella aurita* and *Thalassionema nitzschioides*. The composition of the diatom assemblages suggests that water masses from the cold East Greenland and East Icelandic currents still had a strong influence on the North Icelandic shelf. The assemblages, however, also reveal an influx of the warm Irminger Current and mixing of the cold and warm water masses in the region. The more westerly core site HM107-04 was more influenced by the warm currents than HMI07-05 during the overlapping period.

6.2. The Holocene

6.2.1. Zone D5D, HM107-05 (11150–10100 cal yr BP); Zone D4B, HM107-04 (11110, i.e. top hiatus–9600 cal yr BP)

These early Holocene zones are characterised by abundant *Thalassiosira* sp. resting spores (Fig. 10 and Fig. 11), which may reflect an environment of highly stratified water masses. The lower part of zone D5D contains relatively abundant sea-ice species, while the assemblages in the upper part indicate higher water temperatures. A rapid decrease in the sea-ice species *Fragilariopsis cylindrus* through the zone suggests a climatic amelioration since around 11100 cal yr BP, although there were still abundant cold water diatoms such as *Thalassiosira antarctica* and *Thalassiosira* sp. resting spores. *Fragilariopsis oceanica* and *T. antarctica* resting spores peak at around 10700 cal yr BP in both cores, suggesting a short period of sea surface cooling, while the succeeding appearance of the two warm species *Thalassionema nitzschioides* and *Paralia sulcata* at about 10400 cal yr BP in zone D5D indicates the first marked influence of the warm Irminger Current in the area at about 200 years before the deposition of the Saksunarvatn ash. The climatic warming set in slightly earlier at the more westerly site HMI07-04. In general, there is a lower content of the typical sea-ice species *F. cylindrus* and *F. oceanica* in core HMI07-04 than in core HMI07-05 in the early Holocene, suggesting that slightly warmer water masses prevailed at core site HMI07-04.

6.2.2. Zone D5E, HM107-05 (10100–5100 cal yr BP); Zone D4C, HM107-04 (9600–6000 cal yr BP)

The diatom assemblages in these zones are composed mainly of warm species, and cold water diatoms as well as sea-ice diatoms reach their lowest frequency levels (Fig. 10 and Fig. 11). These assemblages document the strongest influence of the Irminger Current for the entire sedimentary record. However, there appear to be several short cold phases, indicated by a slight increase in sea-ice species and cold species, during this period of time. A peak at around 8700 cal yr BP in core HM107-05 is especially pronounced, where a contemporaneous increase in *Fragilariopsis cylindrus*, *Fragilariopsis oceanica* and *Thalassiosira antarctica* resting spores is seen.

6.2.3. Zone D5F, HM107-05 (5100 cal yr BP to the present); Zones D4D, D4E and D4F, HM107-04 (6000–3150, 3150–1300 and 1300 cal yr BP to the present)

These late Holocene zones are distinguished from the previous interval by a decrease or an almost total disappearance of the Atlantic water indicator *Thalassiosira oestrupii* (Fig. 10 and Fig. 11). A slight increase is observed in the sea-ice species *Fragilariopsis oceanica* as well as the arctic *Thalassiosira antarctica* resting spores. These assemblages show that the influence of the warm Irminger Current had decreased compared to the previous zone, and that a climatic cooling had occurred.

7. Palaeoceanographic changes

The oceanographic circulation north of Iceland was different from the present oceanic system both during the Lateglacial and the Preboreal (Eiríksson et al., 2000a). During certain intervals of the Lateglacial, Atlantic water, presumably related to the strength of the Irminger Current, appears to have had an even stronger influence on the North Icelandic shelf than at any time during the Holocene. The present-day oceanographic current system in the area appears to have been established at about 10200 cal yr BP (e.g. Eiríksson et al., 2000a,b; Knudsen and Eiríksson, 2002).

7.1. The Lateglacial (15740–11500 cal yr BP)

In general, the data show that Polar or Arctic surface water masses were dominant on the North Icelandic shelf throughout the Lateglacial (Fig. 12). This is reflected by the high dominance of *Neogloboquadrina pachyderma* sinistral (>95% of the total planktonic assemblage) and by a high amount of the arctic diatom *Thalassiosira antarctica* resting spores as well as the diatom sea-ice species *Fragilariopsis cylindrus* and *F. oceanica* (see also Fig. 10 and Fig. 11). In some intervals, there is a clear correlation between the amount of diatom sea-ice species and the IRD concentration, i.e. at the base of the record and during the Younger Dryas, but in other intervals they show opposite trends. This is probably due to the fact that the sea-ice may have different origin.
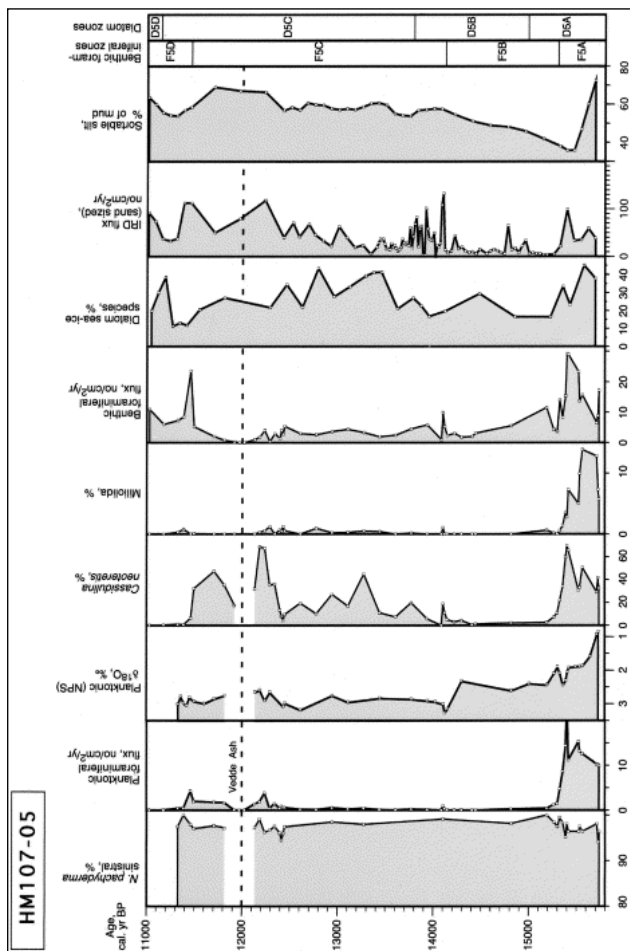

Fig. 12. Data from the time interval between 15800 (bottom of core) and 11000 cal yr BP in core HM107-05. The following parameters are shown on a calibrated time scale: *Neogloboquadrina pachyderma* sinistral (calculated as percentage of total planktonic contents), planktonic foraminiferal flux (number/cm^2/yr), the δ^{18}O of *N. pachyderma* sinistral (NPS, corrected for the ice volume effect), the percentages of the benthic taxa *Cassidulina neoteretis* and Miliolida (calculated as percentages of total benthic contents), the benthic foraminiferal flux (number/cm^2/yr), the percentage of sea-ice diatoms (for species, see text), IRD flux (number/cm^2/yr), and sortable silt content. For comparison, the benthic foraminiferal zonation and the diatom zonation are shown. For stratigraphical correlation, see Fig. 15.

A surface freshwater pulse in this shelf area is reflected by extremely low planktonic oxygen isotope values (NPS) at the base of the sequence (Fig. 8 and Fig. 12). This is especially pronounced between 15740 and 15300 cal yr BP, but continues until about 14300 cal yr BP. Low benthic oxygen isotope values show that brine formation seems to have been active during the same period of time (Fig. 8). One could argue that the low benthic and planktonic δ^{18}O values were due to warm subsurface water flowing into the region north of Iceland in an anti-estuarine circulation mode. Such arguments were proposed by Sarnthein et al. (1995) and Rasmussen et al., 1996 and Rasmussen et al., 1997. However, if one calculates the ice volume corrected amplitude, the 2‰ benthic δ^{18}O lowering at 15700 relative to 15000 cal yr BP would in this scenario imply that the bottom waters of the site were 8°C warmer at 15700 than at 15000 cal yr BP, using a relationship of 0.26‰ per degree C (Shackleton, 1974). Such a warm signal is very unlikely. The brine formation interpretation is also supported by the corresponding negative planktonic δ^{18}O values occurring together with a strong dominance of polar planktonic foraminifera. Inflowing warm intermediate waters can thus be ruled out as a sole explanation for the negative oxygen isotope values, and the brine mechanism is considered to be the only plausible explanation.

The interval between 15740 and 15300 cal yr BP is, however, also characterised by a high amount of benthic Atlantic water indicators such as the opportunistic species *Cassidulina neoteretis* and *Alabaminella weddellensis* together with Miliolida, and there is a clear sedimentological indication of increased bottom water velocities (see also Eiríksson et al., 2000a). This is in accordance with the observation by Hayward et al. (2002), who found that *A. weddellensis* is connected to areas of high mud content receiving a lateral flux of organic matter, i.e. regions with relatively strong bottom currents. Thus, there is indication of a pronounced influence of high-salinity Atlantic waters from the Irminger Current at the seafloor. A mixing of water masses in the area is reflected by high fluxes of both planktonic and benthic foraminifera and by the co-occurrence of diatom sea-ice species and the relatively warm diatom species *Thalassiothrix longissima* (Fig. 10 and Fig. 12).

After a period of generally cold conditions, with dominance of the East Icelandic Current but with some influence of the Irminger Current between 15300–12400 cal yr BP (see also Eiríksson et al.,

2000a), a major oceanic change occurred a few hundred years before the deposition of the Vedde Ash, prevailing until about 11500 cal yr BP. A marked increase is seen in the production of planktonic foraminifera at both sites (Fig. 8, Fig. 9 and Fig. 12), and on the western side of the Kolbeinsey Ridge, the benthic production also went up (HMl07-04). The percentages of the benthic Atlantic water indicator *Cassidulina neoteretis* increase considerably in this interval around the Vedde Ash (Fig. 12). In addition, there is a decrease in oxygen isotope values both for the planktonic (NPS) and for the benthic foraminifera. This presumably indicates a return to a similar environment as seen before 15300 cal yr BP, but less pronounced, i.e. a melt water pulse, brine formation and faunal indication of mixing of the cold surface waters with the underlying Altantic waters. Relatively strong bottom currents were also indicated by the sortable silt percentage in this interval (see also Eiríksson et al., 2000a).

The diatoms indicate continuous arctic surface water conditions through the Lateglacial with long periods of seasonal sea-ice, reflected by the dominance of sea-ice species and arctic diatoms. Similar conditions continued well into the Preboreal. Furthermore, abundance of *Thalassiosira* sp. resting spores around the Vedde Ash horizon corresponds closely to the change in foraminiferal assemblages and the change to light oxygen isotope values mentioned above and continues to form a considerable part of the diatom assemblages until about 9500 cal yr BP, i.e. well into the Holocene, suggesting local stratification of the water masses.

7.2. The Holocene (11500 cal yr BP to the present)

The environmental conditions during the Preboreal north of Iceland appear to have been very different from those of the remaining Holocene. The amount of planktonic foraminifera was very restricted. Almost all specimens belong to the arctic water indicator *Neogloboquadrina pachyderma* sinistral, but the numbers were usually too small for quantitative analyses. There was an increase in benthic foraminiferal flux, however, already at the transition to the Holocene (Fig. 12), with assemblages indicating very cold bottom water conditions, presumably influenced by the NSDW (see Eiríksson et al., 2000a). A benthic faunal change to more diverse assemblages, gradually containing more high-salinity species, reflects a gradual change to an increased influence of Atlantic waters brought to the seafloor with the Irminger Current. This change corresponds to a gradual change to heavier benthic oxygen isotopic values through the Preboreal (Fig. 8).

The continued high amount of diatom sea-ice species and the abundance of *Thalassiosira* sp. resting spores indicate cold freshwater influenced surface water conditions and a strong stratification during the Preboreal. This coincides with a high flux of IRD throughout the Preboreal. Slight climatic amelioration after about 11100 cal yr BP was indicated by the first appearance of diatom species associated with Atlantic water from about 10400 cal yr BP (Fig. 10 and Fig. 11). Planktonic foraminifera return to the area shortly after that (at 10200 cal yr BP; Fig. 9), for the first time with a high amount of subarctic species (<50% *Neogloboquadrina pachyderma* sinistral).

The change in foraminiferal and diatom assemblages and a sharp decrease in IRD flux shortly before the deposition of the Saksunarvatn ash at 10200 cal yr BP (Fig. 9, Fig. 10 and Fig. 11; see also Eiríksson et al., 2000a) indicates the establishment of the modern oceanic circulation pattern in the region. At the same time, increased current velocities at the seafloor are indicated by a distinct rise in sortable silt content on both sides of the Kolbeinsey Ridge. Generally warm, but fluctuating sea surface temperatures are reflected in the foraminiferal and diatom data through the Holocene climatic optimum, i.e. until about 7000 cal yr BP. Temperatures of up to 2–3°C higher than at present in the area are indicated by a high amount of subarctic planktonic foraminifera (from <50 up to about 80% *Neogloboquadrina pachyderma* sinistral; Fig. 9) and by maximum numbers of the warm water diatom *Thalassiosira oestrupii* (Fig. 10 and Fig. 11) in this interval. In addition to minor coolings, one major period of cooling, corresponding to the 8200 cal yr BP event in the Greenland ice cores (i.e. Johnsen et al., 1992), is registered both in the planktonic foraminiferal data and in the diatom assemblages (Fig. 9, Fig. 11 and Fig. 13). According to the percentages of the sinistrally coiled *N. pachyderma*, this cooling of about 3°C appears to be the culmination of a general cooling since about 9000 cal yr BP. The actual cold event appears to have lasted for about 600 years (8600–8000 cal yr BP), according to the age model used here. This general climatic pattern of the Holocene optimum, including the changes during the interval 8600–8000 cal yr BP, is supported by the planktonic δ^{13}C results, where low values are interpreted as indications of more Atlantic water influence, while heavier values are indicative of Arctic water influence (Fig. 9 and Fig. 13). The planktonic oxygen isotope record shows generally low values (2.1–2.6‰) through the cooling event (Fig. 13). The values especially fluctuate at the beginning and close to the end of the event, and the extremely low peaks presumably indicate influx of low-salinity Polar waters in the area. The two periods of fluctuations correspond to peaks in diatom sea-ice species.
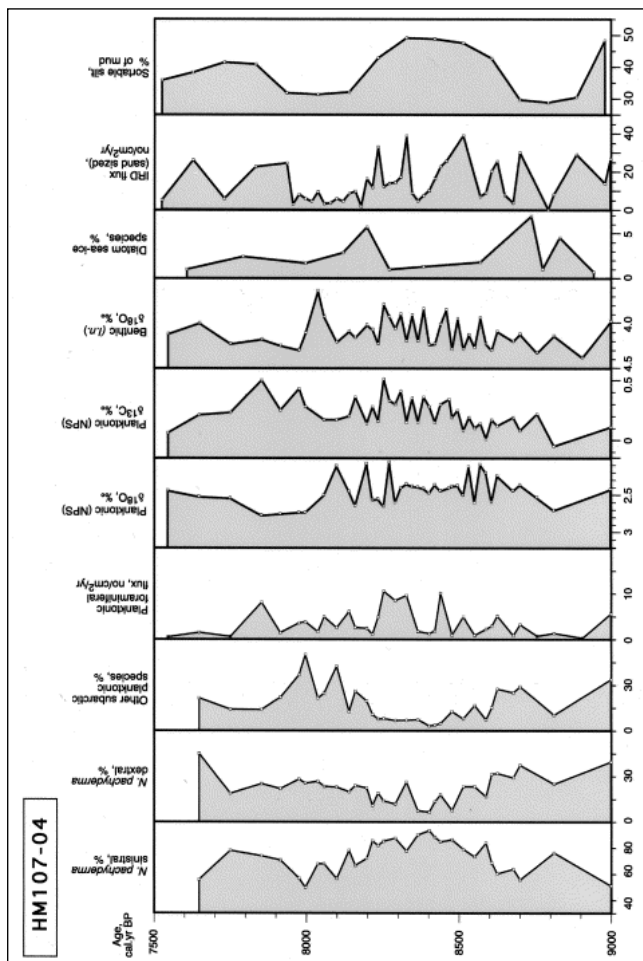

Fig. 13. Data from the time interval between 9000 and 7500 cal yr BP in core HM107-04 (within the foraminiferal zone F4C). The following parameters are shown on a calibrated time scale: *Neogloboquadrina pachyderma* sinistral, *N. pachyderma* dextral (calculated as percentages of total planktonic contents) and other planktonic species, including the following subpolar species: *Turborotalita quinqueloba*, *Globigerina bulloides* and *Globigerinita glutinata*, as well as planktonic foraminiferal flux (number/cm^2/yr), the δ^{18}O records (corrected for the ice volume effect) of the planktonic *N. pachyderma* sinistral (NPS) and the benthic *Islandiella norcrossi* (I.n.), the δ^{13}C of the planktonic *N. pachyderma* sinistral, the percentage of sea-ice diatoms (for species, see text), the IRD flux (number/cm^2/yr) values and the sortable silt content.

The 8600–8000 cal yr BP cooling event, as recorded at core site HM107-04 west of the Kolbeinsey Ridge, coincides with a period of increased sortable silt content (Fig. 14), and the sortable silt mean value is also higher than immediately before and after the event (Fig. 15). IRD flux values are relatively stable before and after the event, i.e. at around 10–15 grains/cm^2/yr, but during the event there are several peaks reaching around 40 grains/cm^2/yr. The 8600–8000 cal yr BP cooling event coincides with quite distinct peaks in the flux values for the two benthic species *Cibicides lobatulus* and *C. neoteretis* (Fig. 14). The *C. lobatulus* increase is probably related to a period of increased bottom currents, with the *C. neoteretis* peak indicating the influence of Atlantic water. This suggests a strongly stratified water column in the area during the cooling event. The relatively poor sorting of the sediment at this level is probably due to the increased sand content, including both the IRD material and the
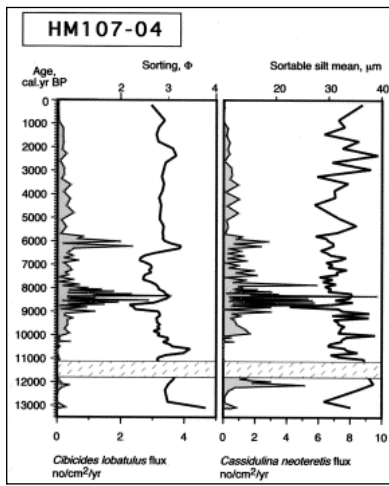
foraminiferal tests.

Fig. 14. The flux (number/cm2/yr) of the benthic species *Cibicides lobatulus* and *Cassidulina neoteretis* plotted against age for core HM107-04. Note prominent flux peaks at around 8200 and 6000 cal yr BP. The standard deviation (sorting in • units) of the total grain size distribution and the sortable silt mean grain size are also shown.
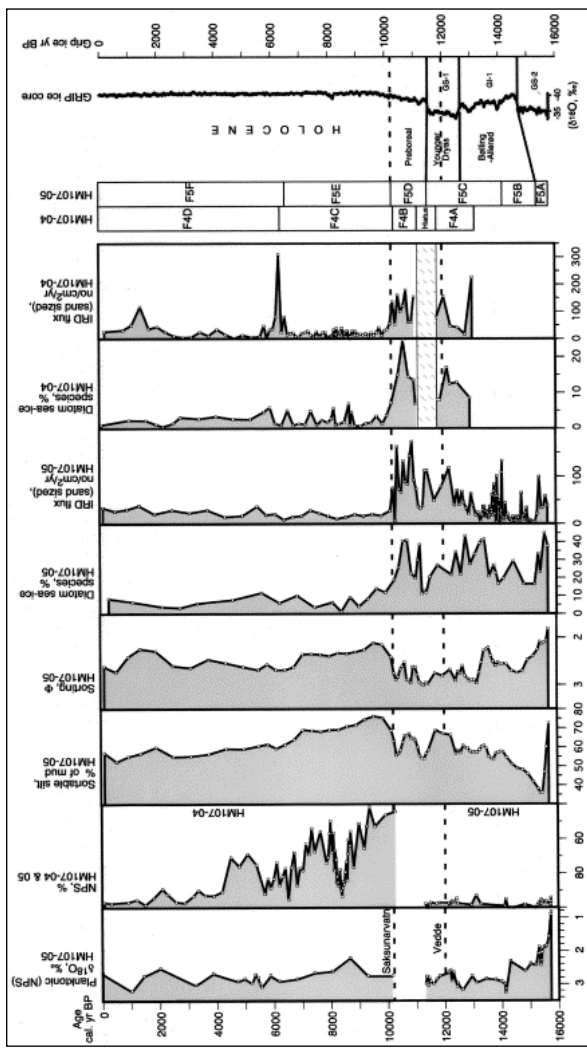

Fig. 15. Comparison of the results from the Lateglacial and Holocene records off North Iceland with the oxygen isotope record of the GRIP ice core (Johnsen et al., 1992 and Johnsen et al., 1995). The Greenland ice-core events (e.g. Björck et al., 1998) are indicated as well as the chronostratigraphical units of Mangerud et al. (1974). The percentages of sinistrally coiled *Neogloboquadrina pachyderma* (NPS) are shown in a combined diagram for the Lateglacial part of HM107-05 and for the Holocene part of HM107-04, while the oxygen isotope record, the contents of diatom sea-ice species, as well as selected sedimentological parameters are shown for each core. The benthic foraminiferal zonation of cores HM107-04 and HM107-05 are included for correlation. Important tephra markers (the Vedde and Saksunarvatn tephras) are shown. For details on the late Holocene climatic oscillations, see Eiríksson et al. (2000b), Jiang et al. (2002) and Knudsen and Eiríksson (2002).

Both the foraminiferal and the diatom data show a general, but fluctuating, cooling since about 7000–6000 cal yr BP. West of the Kolbeinsey Ridge (HM107-04; Fig. 9), a cooling period is reflected between 6500 and 5500 cal yr BP by the planktonic foraminiferal record. This coincides with distinct peaks in the IRD flux in both cores at around 6000 cal yr BP (Fig. 4 and Fig. 5). This is especially pronounced in core HM107-04, where flux peaks in the benthic foraminiferal species *Cibicides lobatulus* and *C. neoteretis* are also notable (Fig. 14). A period of increased stratification of water masses is inferred. The similarity between this interval and the 8600–8000 cal yr BP cooling event is also revealed by the less sorted sediment (increase of sand fraction) and a slightly increased mean sortable silt size. The amount of sortable silt decreases markedly after the 6000 cal yr BP cooling event. According to the foraminiferal data, the cooling event was followed by a relatively warm period between 5500 and 4500 cal yr BP, data which are in accordance with the temperature fluctuations recorded from the GISP2 ice core (O'Brien et al., 1995).

The general trend in the Holocene palaeoceanographic development of the area appears to be comparable in the sedimentary basins on both sides of the Kolbeinsey Ridge, even though both the foraminifera and the diatoms show that the influence of the relatively warm Irminger Current was higher west of the ridge than on the eastern side. At core site HM107-04, generally weak bottom currents are indicated by a low but variable sortable silt content and mean grain size in the Holocene part of the record, reflecting a primarily depositional environment. The grain size data and observed current laminations at site HMl07-05, east of the Kolbeinsey Ridge, indicate a livelier and more efficient circulation regime, accompanied by lower sedimentation rates. This difference may be related to the local topography.

The mean differences in oxygen isotope values (planktonic as well as benthic) to the west and to the east of the Kolbeinsey Ridge, respectively, have been calculated for the period in which the modern oceanographic circulation system has prevailed in the region, i.e. since 10200 cal yr BP. The mean planktonic value (NPS) west of the ridge was 2.52‰ (84 measurements), while the corresponding value east of the ridge was 2.80‰ (21 measurements). This difference supports the faunal indication of continuously higher sea surface temperatures in the western part, even though a difference in salinity may be even more important for the isotopic values. A high influence of the Irminger Current in the western part of the area would increase the oxygen isotope values due to higher salinity and, thus, reduce the apparent temperature difference. The corresponding benthic values (*Islandiella norcrossi*) are 4.11‰ (99 measurements) west of the ridge and 4.19‰ (32 measurements) east of the ridge. Since the benthic foraminiferal assemblages clearly indicate higher temperatures in the western basin, these oxygen isotope values must be highly influenced by increased salinity from the Irminger Current, which particularly influences the bottom waters to the west.

The benthic to planktonic δ^{13}C gradients are similar on both sides of the Kolbeinsey Ridge, indicating a similar degree of surface to bottom stratification. The gradient is also relatively stable through the Holocene.

8. Comparison and discussion

The interval from the bottom of the record at 15740 cal yr BP to the abrupt change in foraminiferal and diatom assemblages as well as in both oxygen and carbon isotope values at about 15300 cal yr BP (13100 ^{14}C years BP) is correlated to the Greenland Stadial 2 (GS-2), i.e. the pre-Bølling. At the beginning of the Bølling Interstadial, a high influx of warm and salty water into the eastern North Atlantic presumably coincided with intensified deep-water formation in the Nordic Seas (e.g. Boyle and Keigwin, 1987; Kroon et al., 1997 and Austin and Kroon, 2001), a change which corresponds to the end of the Heinrich 1 event in the North Atlantic. Grousset et al. (2001) dated the end of the Heinrich 1 event to about 13400 ^{14}C years BP (15700 cal yr BP), while Sarnthein et al. (1999) found that the end of the Heinrich 1 melt water and IRD signals occurred between 13000 and 13400 ^{14}C years BP. According to the GRIP ice-core record, the age of the transition between GS-2 and GI-le (the Bølling Interstadial) is considerably younger than recorded in the North Iceland shelf cores, i.e. at 14700 years (Björck et al., 1998 and Walker et al., 1999). New evidence on very high marine reservoir ages in the North Atlantic at the end of the Heinrich 1 event (Waelbroeck et al., 2001) may help to explain this difference in dating of the transition to the Bølling Interstadial. A correlation of the North Icelandic shelf records with the isotopic record of the GRIP ice core is shown in Fig. 15.

The Heinrich 1 melt water event has previously been recorded off North Iceland by Voelker et al. (1998) and by Sarnthein et al. (1999), and a strong pre-Bølling Irminger Current into this area has also previously been described by Voelker et al. (1998) and by Eiríksson et al. (2000a). The present study clearly supports the idea of an anti-phase temperature relationship between the North Icelandic shelf and the eastern North Atlandic during pre-Bølling time (see also Sarnthein et al., 1995). A subsequent cooling north of Iceland, which is especially pronounced for bottom waters, corresponds to the onset of the Norwegian Sea deep water formation. This would indicate that high influx of Atlantic waters into the eastern North Atlantic led to a reduced Irminger Current north of Iceland. This weakening may reflect an overreaction following a sudden revival of thermohaline circulation into the eastern Nordic Seas after a shutdown state caused by light surface melt water.

On the Southwest Icelandic shelf, however, the Bølling Interstadial is characterised by an influx of relatively warm Irminger Current foraminiferal species (Jennings et al., 2000). Apparently, the northern boundary of the GI-l (Bølling–Allerød) oceanographic warming was to the west and south of the North Icelandic shelf.

The transition from the Bølling–Allerød Interstadial (GI-l) to the Younger Dryas Stadial (GS-1) is not clearly detectable in our data from the cores north of Iceland. This suggests that the temperature change north of Iceland was only minor compared to the abrupt temperature drop recorded in the eastern North Atlantic at the beginning of the Younger Dryas by e.g. Koç Karpuz and Jansen (1992), Haflidason et al. (1995), Kroon et al. (1997) and Klitgaard-Kristensen et al. (2001). A similar relatively warm Younger Dryas was also described by Björck et al. (2002) from Lateglacial lake sediments in southern Greenland and by Kuijpers et al. (2003) from the Southeast Greenland margin. Foraminiferal assemblages from a core on the Southwest Icelandic shelf, however, revealed a marked cooling, at least during the early part of the Younger Dryas (Jennings et al., 2000).

The assemblages and the oxygen isotope values around the level of the Vedde Ash in the two cores north of Iceland indicate a temporary high influence of the Irminger Current as well as a surface melt water peak accompanied by brine formation in the area. The signals are similar to those found in the pre-Bølling, but weaker. An increased influx in boreal benthic foraminiferal species during the later part of the Younger Dryas is also reported from the Southwest Icelandic shelf (Jennings et al., 2000).

The abrupt cooling of both surface and bottom waters north of Iceland at the beginning of the Preboreal (11500 cal yr BP) occurs at exactly the same time as a pronounced warming in the eastern North Atlantic (e.g. Hald and Hagen, 1998 and Klitgaard-Kristensen et al., 2001; at 11400 and 11500 cal yr BP, respectively) and increased deep water formation in the Nordic Seas. Again, this shows that a strong inflow of Atlantic water into the eastern Atlantic apparently coincides with a reduced Irminger Current around Iceland and a strong influence of Norwegian Sea Deep Water on the benthic assemblages north of Iceland. A marked sea surface cooling at around 10700 cal yr BP on the North Icelandic shelf might correspond to the 11000 cooling event as known from the Greenland ice cores (e.g. Björck et al., 1998 and Lowe et al., 2001).

The general consensus seems to be that the establishment of modern sea surface circulation in the northern North Atlantic occurred at about 10000 cal yr BP. For instance, Bauch et al. (2001) concluded that the freshwater input to the central Nordic Seas from melting icebergs completely ceased at that time. Supported by a strong atmospheric warming, the improved sea surface conditions persisted until about 6000 cal yr BP. Similar ages for the Holocene optimal conditions (9000–5000 ^{14}C years BP) were recorded from the Nordic Seas by Koç Karpuz and Schrader (1990), Koç Karpuz and Jansen (1992) and Koç et al. (1993).

The results from the Nordic Seas correspond generally to those from the North Icelandic shelf, which indicate a Holocene climatic optimum between 10200 and 7000–6000 cal yr BP. Bauch et al. (2001), however, found that the maximum temperatures were reached at about 7000 cal yr BP in the central Nordic Seas. The planktonic foraminiferal record off North Iceland would suggest a general temperature decrease between 10200 and 7000 cal yr BP, while the diatom data show fairly consistently high temperatures between 10000 and 7000 cal yr BP. Results of a study of the coccolith distribution in a near-shore core north of Iceland (Andrews and Giraudeau, 2002) also suggest that the Holocene climatic optimum in that area occurred between 10000 and 7000–6000 cal yr BP. This was indicated by the influx of North Atlantic Drift coccolith species to the region, with the highest input during the early part of that period.

It is interesting to note that a Holocene maximum in the northward position of the Intertropical Convergence Zone (titanium and iron concentration data as proxy for on-shore precipitation) was reached in the Cariaco Basin as early as 10500 cal yr BP (Haug et al., 2001). The 'thermal maximum' lasted until 5400 cal yr BP in that area, but with a decreasing trend since about 7000 cal yr BP, indicating similarities between the tropics and the Iceland region. A palaeotemperature reconstruction from the GRIP ice-core record in Greenland, however, indicates optimum temperatures for the Holocene between about 8600 and 4300 yr BP (Johnsen et al., 2001), which is considerably later than indicated by sea surface temperature reconstructions. The ice-core data suggest a temperature drop by 4–8°C during the 8200 cal yr BP event above central Greenland (Johnsen et al., 2001). Planktonic foraminiferal data north of Iceland indicate surface water cooling of about 3°C, while transfer function calculation based on diatoms indicate a summer sea surface temperature drop of about 2°C (Jiang et al., in prep.). The actual background for the 8200 cal yr BP cooling event is not fully understood, but it has been suggested by many authors that fresh melt water input from the Laurentide ice sheet may have influenced the thermohaline system at that time (Klitgaard-Kristensen et al., 1998; Klitgaard-Kristensen et al., 2001; Bianchi and McCave, 1999 and Bauch et al., 2001).

The present Holocene data show a persistent difference between the surface water masses as well as the bottom water masses on each side of the Kolbeinsey Ridge, which has formed a partial barrier between different water masses in the outer shelf area since the last glaciation. The core HM107-05 record on the east side is highly influenced by cold water masses, while the core HM107-04 site west of the ridge has continuously been influenced by an input of Atlantic water from the Irminger Current.

In a study of modern distribution of benthic foraminifera, Rytter et al. (2002) demonstrated how the Kolbeinsey Ridge also acts as an oceanographic barrier for the present benthic assemblages. A similar difference was, however, not seen in the modern diatom distibution in the area (Jiang et al., 2001). Both the modern foraminiferal data and the modern diatom data showed the importance of the position of the oceanic Polar Front for the assemblage distributions. The temporal variations in sea surface temperatures through the Holocene records are supposed to be caused by fluctuations in the position of the marine Polar Front across the area.

9. Summary and conclusions

The data from the North Icelandic shelf allow us to reconstruct the environmental changes since about 15740 cal yr BP. Significant changes are found through the Lateglacial record, with fluctuating influence of the Atlantic water masses of the Irminger Current and Polar water masses deriving from the East Greenland Current.

The isotopic signal reveals that a marked freshwater event, presumably with pronounced brine formation, occurred in the area north of Iceland, being pronounced in pre-Bølling time (before 15300 cal yr BP, corresponding to the Greenland Stadial 2, GS-2), but continuing into the Bølling Interstadial (until about 14300 cal yr BP, i.e. into the Greenland Interstadial 1, GI-1). The foraminiferal and diatom assemblages reflect cold sea surface water masses and a mixing with underlying Atlantic water masses from the Irminger Current during this period. The influence of the Irminger Current was especially strong before 15300 cal yr BP, but there was a continuous, but less strong influence during the entire Bølling–Allerød (GI-1) and the Younger Dryas (GS-1).

A less pronounced melt water event with brine formation, spanning a few hundred years, occurred in the Younger Dryas. The Vedde Ash was deposited as primary tephra within this interval. This melt water event also appears to have been accompanied by a temporary increase in the influence of the Irminger Current in subsurface waters on the North Icelandic shelf. There is no indication of significant cooling in the area during the Younger Dryas.

Very low surface water temperatures and a stratified water column characterise the Preboreal, though with gradually ameliorating conditions both in the surface waters and in the bottom waters towards the end of the Preboreal. A pronounced cooling event is recorded in the diatom data at around 10700 cal yr BP.

The present study supports previous results of a strong palaeo-Irminger Current, which carried warm water masses around Iceland during pre-Bølling time (corresponding to the Heinrich 1 event) and again, but less pronounced, during part of the Younger Dryas. This corresponds to periods of reduced inflow of Atlantic waters into the eastern North Atlantic. Correspondingly, there was a reduced inflow of Irminger Current waters to the North Icelandic shelf during the Bølling Interstadial and during the Preboreal, when, on the other hand, a strong Atlantic Current brought warm water masses into the eastern North Atlantic.

The Lateglacial and Preboreal anti-phase relationship between the environmental indications north of Iceland compared to those in the eastern Atlantic appears to change to an in-phase relationship during the remaining part of the Holocene, at least with respect to the long-term and millennial scale changes.

Planktonic foraminifera show that the modern oceanographic sea surface circulation was established just prior to deposition of the Saksunarvatn tephra at 10200 cal yr BP. This interpretation is supported by a decrease in benthic δ^{13}C values, a drop in IRD fluxes and the first immigration of warm water diatoms.

Generally warm, but fluctuating, sea surface conditions prevailed through the Holocene climatic optimum (between 10200 and 7000–6000 cal yr BP). This was interrupted by a major cooling event between 8600 and 8000 cal yr BP, covering a time span of about 600 years. The cooling is correlated to the 8200 cal yr BP cooling event recorded in the Greenland ice-core records. Another distinct cooling, culminating around 6000 cal yr BP, is followed by a relatively long warm period between about 5500 and 4500 cal yr BP, which is again succeeded by a general, but fluctuating, cooling leading to the present-day conditions. The maximum Holocene foraminiferal fluxes are found in the time interval between about 9000 and 6000 cal yr BP.

Through the entire period since 10200 cal yr BP, the planktonic oxygen isotope values remained lower on the western side of the Kolbeinsey Ridge than on the eastern side. This supports the faunal and floral indication of an eastward decreasing influence of the Irminger Current in that area.

Only minor changes have occurred in the general sea surface circulation system around Iceland during the late Holocene. The time resolution is not high enough in this study to pick up details in this part of the record.

Acknowledgements

References

Andersen, G.J., Heinemeier, J., Nielsen, H.L., Rud, N., Johnsen, S., Sveinbjörnsdóttir, Á.E. and Hjartarson, Á., 1989. AMS ^{14}C dating on the Fossvogur sediments, Iceland. *Radiocarbon* **31**, pp. 592–600.

Andrews, J.T., Hardardóttir, J., Helgadóttir, G., Jennings, A.E., Geirsdóttir, Á., Sveinbjörnsdóttir, Á.E., Schoolfield, S., Kristiansdóttir, G.B., Smith, L.M., Thors, K. and Syvitski, J.P.M., 2000. The N and W Iceland Shelf: Insights into Last Glacial Maximum ice extent and deglaciation based on acoustic stratigraphy and basal radiocarbon AMS dates. *Quat. Sci. Rev.* **19**, pp. 619–631.

Andrews, J.T., Kristjánsdóttir, G.B., Geirsdóttir, Á., Hardardóttir, J., Helgadóttir, G., Sveinbjörnsdóttir, Á.E., Jennings, A.E., Smith, L.M., 2001a. Late Holocene (~5 cal ka) trends and century-scale variability of N. Iceland marine records: Measures of surface hydrography, productivity, and land/ocean interactions. In: Seidov, D., Maslin, M., Haupt, B. (Eds.), The Oceans and Rapid Climate Change: Past, Present and Future. Geophysical Monograph 126, American Geophysical Union, pp. 69–81.

Andrews, J.T., Helgadóttir, G., Geirsdóttir, Á. and Jennings, A.E., 2001. Multicentury-scale records of carbonate (hydrographic?) variability on the Northern Iceland Margin over the last 5000 yrs. *Quat. Res.* **56**, pp. 199–206.

Andrews, J.T., Caseldine, C., Weiner, N. and Hatton, J., 2001. Late Holocene (ca. 4 ka) marine and terrestrial environmental change in Reykjarfjördur, north Iceland: Climate and/or settlement?. *J. Quat. Sci.* **16**, pp. 133–143.

Andrews, J.T. and Giraudeau, J., 2002. Multi-proxy records showing significant Holocene environmental variability: The inner N. Iceland shelf (Húnaflói). *Quat. Sci. Rev.* **22**, pp. 175–193.

Austin, W.E.N., Bard, E., Hunt, J.B., Kroon, D. and Peacock, J.D., 1994. The ^{14}C age of the Icelandic Vedde Ash: Implications for Younger Dryas Marine Reservoir Age Corrections. *Radiocarbon* **37**, pp. 53–62.

Austin, W.E.N. and Kroon, D., 2001. Deep sea ventilation of the northeastern Atlantic during the last 15,000 years. *Global Planet. Change* **30**, pp. 13–31.

Bard, E., 1990. Calibration of the ^{14}C timescale over the past 30,000 years using mass spectrometric U–Th ages from Barbados corals. *Nature* **345**, pp. 405–410.

Bard, E., Arnold, M., Mangerud, J., Paterne, M., Labeyrie, L., Duprat, J., Mélieres, M.-A.M., Sønstegaard, E. and Duplessy, J.-C., 1994. The North Atlantic atmosphere–sea surface ^{14}C gradient during the Younger Dryas climatic event. *Earth Planet. Sci. Lett.* **126**, pp. 275–287.

Bauch, H.A., Erlenkeuser, H., Spielhagen, R.F., Struck, U., Matthiessen, J., Thiede, J. and Heinemeier, J., 2001. A multiproxy reconstruction of the evolution of deep and surface waters in the subarctic Nordic seas over the last 30,000 yr. *Quat. Sci. Rev.* **20**, pp. 659–678.

Bianchi, G.G. and McCave, I.N., 1999. Holocene periodicity in North Atlantic climate and deep-ocean flow south of Iceland. *Nature* **397**, pp. 515–517.

Björck, S., Walker, M.J.C., Cwynar, L.C., Johnsen, S., Knudsen, K.-L., Lowe, J.J., Wohlfarth, B., the INTIMATE Members, 1998. An event stratigraphy for the Last Termination in the North Atlantic region based on the Greenland ice-core record: A proposal by the INTIMATE Group. *J. Quat. Sci.* 13, 283–292.

Björck, S., Bennike, O., Rosén, P., Andresen, C.S., Bohncke, S., Kaas, E. and Conley, D., 2002. Anomalously mild Younger Dryas summer conditions in southern Greenland. *Geology* 90, pp. 427–430.

Bondevik, S., Mangerud, J. and Gulliksen, S., 2001. The marine ^{14}C age of the Vedde Ash Bed along the west coast of Norway. *J. Quat. Sci.* 16, pp. 3–7.

Boyle, E.A. and Keigwin, L., 1987. North Atlantic Thermohaline circulation during the last 20,000 years linked to high-latitude surface temperatures. *Nature* 330, pp. 35–40.

De Séve, M.A., 1999. Transfer function between surface sediment diatom assemblages and sea-surface temperature and salinity of the Labrador Sea. *Mar. Micropaleontol.* 36, pp. 249–267.

Dokken, T. and Jansen, E., 1999. Rapid changes in the mode of deep and intermediate water formation linked with atmospheric and ice sheet variations during the Last Glacial. *Nature* 401, pp. 458–461.

Eiríksson, J., Knudsen, K.L., Haflidason, H. and Henriksen, P., 2000. Late-glacial and Holocene palaeoceanography of the North Icelandic shelf. *J. Quat. Sci.* 15, pp. 23–42.

Eiríksson, J., Knudsen, K.L., Haflidason, H. and Heinemeier, J., 2000. Chronology of Late Holocene climatic events in the northern North Atlantic based on AMS ^{14}C dates and tephra markers from the volcano Hekla, Iceland. *J. Quat. Sci.* 15, pp. 573–580.

Ellis, B.F., Messina, A., 1949. Catalogue of Foraminifera (Supplements, including 1998). Am. Mus. Natl. Hist. Micropaleontpl. Press, New York.

Fairbanks, R., 1989. A 17,000-year glacio-eustatic sea level record: Influence of glacial melting rates on the Younger Dryas event and deep-ocean circulation. *Nature* 342, pp. 637–642.

Feyling-Hanssen, R.W., Jørgensen, J.A., Knudsen, K.L. and Andersen, A.-L.L., 1971. Late Quaternary Foraminifera from Vendsyssel, Denmark and Sandnes, Norway. *Bull. Geol. Soc. Den.* 21, pp. 67–317.

Fronval, T. and Jansen, E., 1997. Eemian and early Weichselian (140–60 ka) paleoceanography and paleoclimate in the Nordic seas with comparisons to Holocene conditions. *Paleoceanography* 12, pp. 443–462.

Grimm, E., 1987. CONISS: A Fortran 77 program for stratigraphically constrained cluster analysis by the method of incremental sum of squares. *Comput. Geosci.* 13, pp. 13–35.

Grousset, F.E., Cortijo, E., Huon, S., Hervé, L., Richter, T., Burdloff, D., Duprat, J. and Weber, O., 2001. Zooming in on Heinrich layers. *Paleoceanography* 16, pp. 240–259.

Grönvold, K., Óskarsson, N., Johnsen, S.J., Clausen, H.B., Hammer, C.U., Bond, C. and Bard, E., 1994. Ash layers from Iceland in the Greenland GRIP ice core correlated with oceanic and land sediments. *Earth Planet. Sci. Lett.* 135, pp. 149–155.

Gulliksen, S., Birks, H.H., Possnert, G. and Mangerud, J., 1998. A calendar age estimate of the Younger Dryas–Holocene boundary at Kråkenes, western Norway. *Holocene* 8, pp. 249–259.

Haflidason, H., Sejrup, H.P., Kristensen, D.K. and Johnsen, S., 1995. Coupled response of the Late Glacial climatic shifts of northwest Europe reflected in Greenland ice cores: Evidence from the northern North Sea. *Geology* 23, pp. 1059–1062.

Hald, M. and Hagen, S., 1998. Early Preboreal cooling in the Nordic seas region triggered by meltwater. *Geology* 26, pp. 615–618.

Hansen, B. and Østerhus, S., 2000. North Atlantic–Nordic Seas exchanges. *Prog. Oceanogr.* 45, pp. 109–208.

Hasle, G.R., Syvertsen, E.E., 1997. Marine diatoms. In: Tomas, C.R. (Ed.), Identifying Marine Phytoplankton. Academic Press, CA, pp. 5–385.

Haug, G.H., Hughen, K.A., Sigman, D.M., Peterson, L.C. and Röhl, U., 2001. Southward migration of the Intertropical Convergence Zone through the Holocene. *Science* 293, pp. 1304–1308.

Hayward, B.W., Neil, H., Carter, R., Grenfell, H.R. and Hayward, J.J., 2002. Factors influencing the distribution patterns of Recent deep-sea benthic foraminifera, east of New Zealand, Southwest Pacific Ocean. *Mar. Micropaleontol.* 46, pp. 139–176.

Hendey, N.I., 1964. An introductory account of the smaller algae of British coastal waters, Part V. Bacillariophyceae (diatoms). *Fish. Invest., Lond. Ser.* 4, pp. 1–317.

Henrich, H., Wagner, T., Goldschmidt, P. and Michels, K., 1995. Depositional regimes in the Norwegian–Greenland Sea: The last two glacial to interglacial transitions. *Geol. Rundsch.* 84, pp. 28–48.

Hurdle, B.G. (Ed.), 1986. The Nordic Seas. Springer, New York, 777 pp.

Hustedt, F., 1930–1960. Die Kieselalgen Deutschlands, Österreichs und der Schweiz unter Berücksichtung der übrigen Länder Europas sowie der angrenzenden Meeresgebiete. In: Rabenhorsts, L. (Ed.), Kryptogamen-Flora 7. Akad. Verlag, Leipzig.

Jennings, A., Syvitski, J., Gerson, L., Grönvold, K., Geirsdóttir, Á., Hardardóttir, J., Andrews, J. and Hagen, S., 2000. Chronology and paleoenvironments during the late Weichselian deglaciation of the southwest Iceland shelf. *Boreas* 29, pp. 167–183.

Jiang, H., 1996. Diatoms from the surface sediments of the Skagerrak and the Kattegat and their relationship to the spatial changes of environmental variables. *J. Biogeogr.* **23**, pp. 129–137.

Jiang, H., Björck, S. and Knudsen, K.-L., 1997. A palaeoclimatic and palaeoceanographic record of the last 11000 ^{14}C years from the Skagerrak–Kattegat, northeastern Atlantic margin. *Holocene* **7**, pp. 301–310.

Jiang, H., Seidenkrantz, M.-S., Knudsen, K.L. and Eiríksson, J., 2001. Diatom surface sediment assemblages around Iceland and their relationships to oceanic environmental variables. *Mar. Micropaleontol.* **41**, pp. 73–96.

Jiang, H., Seidenkrantz, M.-S., Knudsen, K.L. and Eiríksson, J., 2002. Late-Holocene summer sea surface temperatures based on a diatom record from the north Icelandic shelf. *Holocene* **12**, pp. 137–147.

Johannesen, O.M., 1986. Brief overview of the physical oceanography. In: Hurdle, B.G. (Ed.), The Nordic Seas. Springer, New York, pp. 103–127.

Johannesen, T., Jansen, E., Flatøy, A., Ravelo, A.C., 1994. The relationship between surface water masses, oceanographic fronts and paleoclimatic proxies in surface sediments of the Greenland, Iceland, Norwegian Seas. In: Zahn, R., Kaminski, M. (Eds.), Carbon Cycling in the Glacial Ocean. NATO ASI Series I, 17, Springer, Berlin, pp. 61–85.

Johnsen, S.J., Clausen, H.B., Dansgaard, W., Fuhrer, K., Gundestrup, N., Hammer, C.U., Iversen, P., Jouzel, J., Stauffer, B. and Steffensen, J.P., 1992. Irregular glacial interstadials recorded in a new Greenland ice core. *Nature* **359**, pp. 311–313.

Johnsen, S., Dahl-Jensen, D., Dansgaard, W. and Gundestrup, N., 1995. Greenland palaeotemperatures derived from GRIP bore hole temperature and ice core isotope profiles. *Tellus* **47B**, pp. 624–629.

Johnsen, S.J., Dahl-Jensen, D., Gundestrup, N., Steffensen, J.P., Clausen, H.B., Miller, H., Masson-Delmotte, V., Sveinbjörnsdóttir, A.E. and White, J., 2001. Oxygen isotope and palaeotemperature records from six Greenland ice-core stations: Camp Century, Dye-3, GRIP, GISP2, Renland and NorthGRIP. *J. Quat. Sci.* **16**, pp. 299–307.

Klitgaard-Kristensen, D., Sejrup, H.P., Haflidason, H., Johnsen, S. and Spurk, M., 1998. A regional 8200 cal. yr BP cooling event in northwest Europe, induced by final stages of the Laurentide ice-sheet deglaciation. *J. Quat. Sci.* **13**, pp. 165–169.

Klitgaard-Kristensen, D., Sejrup, H.P. and Haflidason, H., 2001. The last 18 kyr fluctuations in the Norwegian Sea surface conditions and implications for the magnitude of climatic change: Evidence from the North Sea. *Paleoceanography* **16**, pp. 455–467.

Knudsen, K.L., 1998. Foraminiferer i Kvartær stratigrafi: Laboratorie- og fremstillingsteknik samt udvalgte eksempler. *Geol. Tidsskr.* **3**, pp. 1–25.

Knudsen, K.L. and Eiríksson, J., 2002. Application of tephrochronology to the timing and correlation of palaeoceanographic events recorded in Holocene and Lateglacial shelf sediments off North Iceland. *Mar. Geol.* **191**, pp. 165–188.

Koç Karpuz, N. and Jansen, E., 1992. A high-resolution diatom record of the last deglaciation from the SE Norwegian Sea: Documentation of rapid climatic changes. *Paleoceanography* **7**, pp. 499–520.

Koç Karpuz, N. and Schrader, H., 1990. Surface sediment diatom distribution and Holocene paleotemperature variations in the Greenland, Iceland and Norwegian Sea. *Paleoceanography* **5**, pp. 557–580.

Koç, N., Jansen, E. and Haflidason, H., 1993. Paleoceanographic reconstructions of surface ocean conditions in the Greenland, Iceland and Norwegian seas through the last 14 Ka based on diatoms. *Quat. Sci. Rev.* **12**, pp. 115–140.

Kroon, D., Austin, W.E.N., Chapman, M.R. and Ganssen, G.M., 1997. Deglacial surface circulation changes in the northeastern Atlantic: Temperature and salinity records off NW Scotland on a century scale. *Paleoceanography* **12**, pp. 755–763.

Kuijpers, A., Troelstra, S.R., Prins, M.A., Linthout, K., Akhmetzhanov, A., Bouryak, S., Bachmann, M.F., Lassen, S., Rasmussen, S. and Jensen, J.B., 2003. Late Quaternary sedimentary processes and ocean circulation changes at the Southeast Greenland Margin. *Mar. Geol.* **195**, pp. 109–129.

Lackschewitz, K.S., Dehn, J. and Wallrabe-Adams, H.-J., 1994. Volcaniclastic sediments from mid-oceanic Kolbeinsey Ridge, north of Iceland: Evidence for submarine volcanic fragmentation processes. *Geology* **22**, pp. 975–978.

Lassen, S., Jansen, E., Knudsen, K.L., Kuijpers, A., Kristensen, M., Christensen, K., in press. Bottom water variability in the Faeroe area, NE Atlantic, 30–10 ^{14}C kyr BP – Benthic foraminiferal evidence. Mar. Micropaleontol.

Lowe, J.J., Hoek, W.Z., INTIMATE Group, 2001. Inter-regional correlation of palaeoclimatic records for the Last Glacial–Interglacial transition: A protocol for improved precision recommended by the INTIMATE project group. Quat. Sci. Rev. 20, 1175–1187

Malmberg, S.A. and Jonsson, S., 1997. Timing of deep convection in the Greenland and Iceland Seas. *J. Mar. Sci.* **54**, pp. 300–309.

Mangerud, J., Andersen, S.T., Berglund, B. and Donner, J.J., 1974. Quaternary stratigraphy of Norden, a proposal for terminology and classification. *Boreas* **4**, pp. 109–128.

McBride, E.F., 1971. Mathematical treatment of size distribution data. In: Carver, R.E. (Ed.), Procedures in Sedimentary Petrology. Wiley, New York, pp. 109–127.

McCave, I.N., Manighetti, B. and Robinson, S.G., 1995. Sortable silt and fine sediment size/composition

slicing: Parameters for paleocurrent speed and palaeoceanography. *Paleoceanography* **10**, pp. 593–610.

O'Brien, S.R., Mayewski, P.A., Meeker, L.D., Meese, D.A., Twickler, M.S. and Whitlow, S.L., 1995. Complexity of Holocene climate as reconstructed from a Greenland ice core. *Science* **270**, pp. 1962–1964.

Rasmussen, T.L., Thomsen, E., Labeyrie, L. and van Weering, T.C.E., 1996. Circulation changes in the Faeroe–Shetland Channel correlating with cold events during the last glacial period (58–10 ka). *Geology* **24**, pp. 937–940.

Rasmussen, T.L., van Weering, T.C.E. and Labeyrie, L., 1997. Climatic instability, ice sheets and ocean dynamics at high northern latitudes during the Last Glacial period (58–10 ka BP). *Quat. Sci. Rev.* **16**, pp. 71–80.

Rytter, F., Knudsen, K.L., Seidenkrantz, M.-S. and Eiríksson, J., 2002. Modern distribution of benthic foraminifera on the north Icelandic shelf and slope. *J. Foraminif. Res.* **32**, pp. 217–244.

Sancetta, C., 1981. Oceanographic and ecological significance of diatoms in surface sediments of the Bering and Okhotsk seas. *Deep-Sea Res.* **28**, pp. 789–817.

Sarnthein, M., Jansen, E., Weinelt, M., Arnold, M., Dup1essy, J.-C., Erlenkeuser, H., Flatøy, A., Johannessen, G., Johannessen, T., Jung, S., Koç, N., Labeyrie, L., Maslin, M., Pflaumann, U. and Schulz, H., 1995. Variations in Atlantic surface paleoceanography, 50°–80°N: A time-slice record of the last 30,000 years. *Paleoceanography* **10**, pp. 1063–1094.

Sarnthein, M., Stattegger, K., Dreger, D., Erlenkeuser, H., Grootes, P., Haupt, B., Jung, S., Kiefer, T., Kuhnt, W., Pflaumann, U., Schäfer-Neth, C., Schulz, H., Schulz, M., Seidov, D., Simstich, J., van Krevelt, S., Vogelsang, E., Völker, A., Weinelt, M., 1999. Fundamental modes and abrupt changes in North Atlantic circulation and climate over the last 60 ky – Concepts, reconstruction and numerical modelling. In: Schäfer, P., Ritzrau, W., Schüter, M., Thiede, J., (Eds.), The Northern North Atlantic: A Changing Environment. Springer, Berlin, pp. 45–66.

Shackleton, N.J., 1974. Attainment of isotopic equilibrium between ocean water and the benthonic foraminifera genus *Uvigerina*: Isotopic changes in the ocean during the last glacial. *Colloq. Cent. Natl. Rech. Sci.* **219**, pp. 203–209.

Stefansson, U., 1962. North Icelandic Waters. *Rit Fiskideild.* **3**, pp. 1–269.

Stuiver, M., Reimer, P.J., Bard, E., Beck, J.W., Burr, G.S., Hughen, K.A., Kromer, B., McCormack, G., van der Plicht, J. and Spurk, M., 1998. INTCAL98 Radiocarbon Age Calibration, 24,000–0 cal BP. *Radiocarbon* **40**, pp. 1041–1083.

Stuiver, M., Reimer, P.J. and Braziunas, T.F., 1998. High-precision radiocarbon age calibration for terrestrial and marine samples. *Radiocarbon* **40**, pp. 1127–1151.

Swift, J.H., 1986. The Arctic Waters. In: Hurdle, B.G. (Ed.), The Nordic Seas. Springer, New York, pp. 129–153.

van Andel, T.H., Hearth, G.H. and Moore, T.C., 1975. Cenozoic history and paleoceanography of the central equatorial Pacific. *Mem. Geol. Soc. Am.* **143**, pp. 1–134.

Veum, T., Jansen, E., Arnold, M., Beyer, I. and Duplessy, J.C., 1992. Water mass exchange in the North Atlantic and the Norwegian Sea during the past 28,000 years. *Nature* **356**, pp. 783–785.

Vidal, L., Labeyrie, L. and van Weering, T.C.E., 1998. Benthic $\delta^{18}O$ records in the North Atlantic over the last glacial period (60–10kyr): Evidence for brine formation. *Paleoceanography* **13**, pp. 245–251.

Voelker, A.H.L., Sarnthein, M., Grootes, P.M., Erlenkeuser, H., Laj, C., Mazaud, A., Nadeau, M.-J., Schleicher, M., 1998. Correlation of marine ^{14}C ages from the Nordic Seas with the Gisp2 isotope record: Implications for ^{14}C calibration beyond 25 ka BP. In: Mook, W.G., Plicht, J. van der (Eds.), Proceedings of the 16th International [14]C Conference, Radiocarbon 40, pp. 517–534.

Vogelsang, E., 1990. Paläo-Ozeanographie des Europäischen Nordmeeres an Hand stabiler Kohlenstoff- und Sauerstoffisotopen. *Ber. Sonderforsch.bereich* **313**, pp. 1–136.

Waelbroeck, C., Duplessy, J.-C., Michel, E., Labeyrie, L., Paillard, D., Duprat, J., 2001. The timing of the last deglaciation in North Atlantic climate records. Nature 412, 724–727 and Nature 414, 470 (correction).

Walker, M.J.C., Björck, S., Lowe, J., Cwynar, L.C., Johnsen, S., Knudsen, K.-L., Wohlfarth, B., the INTIMATE Group, 1999. Isotopic 'events' in the GRIP ice core: A stratotype for the Late Pleistocene. Quat. Sci. Rev. 18, 1143–1150.

Zielinski, G.A., Mayewski, P.A., Meeker, L.D., Grönvold, K., Germani, M.S., Whitlow, S., Twickler, M.S. and Taylor, K., 1997. Volcanic aerosol records and tephrochronology of the Summit, Greenland, ice cores. *J. Geophys. Res.* **102**, pp. 26625–26640.

Appendix A. List of foraminiferal taxa

The original descriptions of the foraminiferal taxa cited in the text are reported in Ellis and Messina (1949)

Planktonic taxa:

Globigerina bulloides d'Orbigny, 1826

Globigerinita glutinata (Egger) = *Globigerina glutinata* Egger, 1895

Neogloboquadrina pachyderma (Ehrenberg) = *Aristerospira pachyderma* Ehrenberg, 1861

Turborotalita quinqueloba (Natland) = *Globigerina quinqueloba* Nat1and, 1938

Benthic taxa:

Cassidulina neoteritis Seidenkrantz, 1995 (previously often referred to *Cassidulina teretis*) Tappan, 1951

Cibicides lobatulus (Walker and Jacob) = *Nautilus lobatulus* Walker and Jacob, 1798

Islandiella norcrossi (Cushman) = *Cassidulina norcrossi* Cushman, 1933

Miliolida

Appendix B. List of diatom taxa

(H and S = Hasle and Syvertsen, 1997)

Actinocyclus curvatulus Janish, in A. Schmidt, 1878 (H and S, pl. 21–122)

Fragilariopsis cylindrus (Grunow) Krieger, in Helmcke and Krieger, 1954 (H and S, pp. 302, 305)

Fragilariopsis oceanica (Cleve) Hasle, 1965 (H and S, pp. 299, 305)

Odontella aurita (Lyngbye) Agardh, 1832 (H and S, p. 239)

Paralia sulcata (Ehrenberg) Cleve, 1873 (H and S, p. 91; Hendey, 1964, p. 73)

Rhizosolenia borealis Sundström, 1986 (H and S, pl. 47)

Rhizosolenia hebetata Bailey, 1856 (H and S, pl. 49–150; Hendey, 1964, pp. 150–151)

Thalassionema nitzschioides (Grunow) Mereschkowsky, 1902 (H and S, pp. 257–262; Hendey, 1964, pl. 65)

Thalassiosira antarctica Comber, 1896 (H and S, pp. 66–68, 71)

Thalassiosira nordenskioeldii Cleve, 1873 (H and S, p. 56, 59; Hendey, 1964, p. 85)

Thalassiosira oestrupii (Ostenfeld) Hasle, 1972 (H and S, pp. 83, 86)

Thalassiosira pacifica Gran and Angst, 1931 (H and S, pp. 57, 59)

Thalassiothrix longissima Cleve and Grunow, 1880 (H and S, pp. 263–267)